A Thesis

On

Morphological and dielectric behavior of carbon nanotube-ferroelectric liquid crystal composite

In

Partial fulfillment of the requirements for the award of the degree

Of

MASTER OF TECHNOLOGY

In

MATERIAL SCIENCE & ENGEERING

Submitted By

SIMTA RANI

Roll No. 6050508

Under the guidance of

Professor K.K. Raina

School of Physics & Material Science
Thapar University
Patiala-147004, India

CERTIFICATE

This is to certify that the thesis entitled **"*Morphological and dielectric behavior of carbon nanotube-ferroelectric liquid crystal composite*"** which is being submitted by ***Simta Rani*** in Partial fulfilment of the requirements for the award of the degree of ***Master of Technology (M.Tech.) in Material Science and Engineering*** of Thapar University, Patiala (India), is a record of the study conducted by her under my supervision and guidance and that no part of this thesis has been submitted for the award of any other degree.

Date:
Place:

Dr. K.K. Raina
Deputy Director,
Dean, Faculty
Dean, RPG
Thapar University Patiala

COUNTERSIGNED

Dr. O. P. Pandey

Professor and Head
School of Physics & Material Sciences
Thapar University
Patiala- 147004

Dr. R. K. Sharma

Dean, Academic Affairs
Thapar University
Patiala- 147004

Dedicated

To

My parents

ACKNOWLEDGEMENT

The real spirit of achieving a goal is through the way of excellence and discipline. I would have never succeeded in completing my task without the cooperation, encouragement and help provided to me by various personalities.

With deep sense of gratitude I express my sincere thanks to my esteemed and worthy supervisor Dr. K.K. Raina, Professor, School of Physics and Material Science, who has given the support and encouragement me at every stage of my work. His meticulous attention towards my proceeding, his devoted time and his ideas has enabled me to make this seminar work to success

I shall be failing in my duties if I do not express my deep sense of gratitude towards Dr O.P. Pandey, Professor& Head, School of Physics and Material Science (Thapar University), Patiala who has been a constant source of inspiration for me throughout this seminar work.

I also extend my special gratitude to Mr. Pankaj Kumar, Miss Shikha and Mr. Rakesh Sharma for their constructive suggestions at different stages of this work. My greatest thanks are to all who wished me success.

I am very thankful to my sister, brother and parents for their constant co-operation, inspiration, patience, blessing and moral support.

Above all, I owe my reverence to 'Almighty' for his kindness who blessed me at finish of whole work.

Simta

ABSTRACT

Nanotube dispersed ferroelectric liquid crystals are playing very vital role in the development of new materials for improving display devices in industries. Carbon nanotube dispersed ferroelectric liquid crystals have high dielectric constant, fast switching response, and large electro-optic coefficient, making them ideal for memories, capacitors and display devices etc. In this work, an attempt has been made to understand the influence of carbon nanotubes on dielectric and morphological properties of FLC and how the level (wt/wt%) of carbon nanotubes concentration effect the switching response and transition temperature of FLCs. Introduction to the fundamentals of ferroelectric liquid crystals and effect of nanotubes on properties of FLC has been reviewed.

CONTENTS

CHAPTER 1
Introduction

1.1 REVIEW

Composites based on liquid crystals (LCs) have attracted much attention over last number of years because of their unique electro- and magneto-optic properties and novel display applications. Typical examples of these systems are polymer dispersed liquid crystals [1], suspensions of aerosils in LC matrices [2] and suspensions of nanotubes in ferroelectric LCs [3, 4]. The inclusions in known composite LC systems produce director distortions that extend over macroscopic scales. A new approach, however, was proposed recently by few years [5]. This is based on the idea of controlling the properties of the composites by adding a low concentration of nanotubes into a LC matrix. These dilute nano suspensions are stable due to the weak interactions of the nanotubes at low concentrations. The nanotubes are so small that they do not disturb the LC orientation and thus macroscopically homogeneous structures are obtained. At the same time, the nanotubes are sufficiently large to maintain the intrinsic properties of the materials from which they are made (e.g. ferromagnetism or ferroelectricity) and share these properties with the LC matrix due to anchoring with the LC. In particular, it was found that embedding nanotubes in a ferroelectric liquid crystal at a low volume concentration (0.1%) did not change the elastic and anchoring properties of the LC, but did result in an enhanced dielectric response. In addition, the suspension exhibited an unusual linear response to the electric vector; the direction of the director reorientation was determined by the sign of the applied electric field. Here we report studies of the dielectric properties of a liquid crystal suspension containing carbon nanotubes. We found that embedding the carbon nanotubes in a LC results in changes of the dielectric spectra of the matrix, caused by the strong interaction between LC and carbon nanotubes.

Obtaining stable and uniform alignment of liquid crystal (LCs) on a macroscopic scale is essential to the fabrication of high-quality liquid crystal displays (LCDs). Typically, alignment involves modification of a solid substrate such that its interface with the LC has some anchoring action that results in either planar (tangential) or homeotropic

(perpendicular) orientation of the LC director (symmetry axis) with respect to the interface. Such modification is carried out on a substrate having an electrically conductive layer (usually indium tin oxide or ITO-coated glass) for electric-field-induced reorientation of the director which, in turn, results in a variation in the transmitted light intensity.

Nano-composites (from a fraction of a nanometer to about 100 nm) are at the confluence of the smallest of human-made devices and the largest molecules of living systems. At this dimension scale, nanotubes imbedded in a liquid crystal do not significantly perturb the director field in the liquid crystal and interaction between the nanotubes is weak. However, the nanotubes share their intrinsic properties with the liquid crystal matrix due to alignment and anchoring with the liquid crystal. For instance, it was recently reported that dispersing low concentration of submicron nanotubes in a ferroelectric liquid crystals enhance the dielectric response and induces a linear response to the electric vector E in a ferooelctric liquid crystals [6]. In contrast to molecular additives, these tubes dispersions substantially lower the operating voltage of liquid crystals displays and related devices. Herein, we explore the potential of selfassembled carbon nanotube (CNT) bundles as an alignment substrate for Liquid crystals [7].

Since their discovery [8], carbon nanotubes (CNT) have received immense attention across many disciplines by virtue of their unique structure and properties, as well as possible applications as nano-sensors and devices. Applications of interest include electron-emitting panel displays [9], single-molecular transistors in microelectronics [10], artificial muscles [11], and molecular filtration membranes [12]. An essential prerequisite for realizing the aforementioned applications centers on the fabrication of aligned CNT which has been a focused area of recent research efforts [13-18]. Alignment of nanotubes with the aid of ferroelectric liquid crystals is an alternative approach in which the CNT molecules were found to orient parallel to the director of a ferroelectric solvent [19] observed molecular alignment was attributed to liquid crystal-induced alignment of the CNT.

1.2 FERROELECTRIC LIQUID CRYSTAL

In a theoretical examination of the structures of liquid crystal phases, Robert B. Meyer in 1975 creatively utilized symmetry arguments to predict that tilted, layered liquid crystal phases of chiral molecules are ferroelectric. He then engaged the help of organic chemists to synthesize a compound that might possess such a phase, and once the material was in his hands, Meyer not only verified its ferroelectricity, but also suggested how such a phase could be used for extremely fast displays. This discovery of ferroelectricity in a fluid system with the possibility for unique applications surprised the entire condensed matter research community and quickly paved the way for both increased scientific understanding and significant technological advancement.

This leads to further study of ferroelectric liquid crystals (FLC). In 1980 Clark and Lagerwall published the concept of the Surface Stabilized Ferroelectric Liquid Crystal (SSFLC) device. This was a major step forward in the possibility of useful applications of FLCs. As FLC products became more feasible, the technology became commercialized. The initial products appearing in 1989 were direct-view displays and print bars.

There is still major interest in FLC technology. This is due to the promise of fast switching and high resolution. These advantages and the possibility for dynamic gray scale and full color of SSFLC give it great potential for use in demanding applications such as high definition television (HDTV). The advantages do not come without some complications in production however. These difficulties explain the lack of major commercial breakthroughs in recent years.

FLCs have already been developed for miniature displays. These displays can be magnified or projected for a full screen image. They can also be used in head mounted displays such as those used for virtual reality. Such displays are highly portable and also allow for interactivity with the user (image changes as user's head turns). Since the display is supported by the user, weight is of great importance. The simplest way to reduce the weight of the system is to reduce the size of the screen needed. Meanwhile, the resolution must be high to make the image realistic to the user. FLC displays allow for this by their small pixel sizes. Also, FLCs can use reflective illumination to eliminate

bulky (and high energy consuming) backlighting devices. The bistability offered by SSFLC devices make them ideal where low energy consumption is a concern for still images since additional power is not required once image is created. Yet, their switching time is fast enough to provide high frame rates required for video. The fast switching time also allows full color on each pixel which means higher quality on a display of a given size.

1.2.1 What are liquid crystals?

To those who know that substances can exist in three states, solid, liquid, and gas, the term "liquid crystal" may be puzzling. How can a liquid be crystalline? However, "liquid crystal" is an accurate description of both the observed state transitions of many substances and the arrangement of molecules in some states of these substances.

Many substances can exist in more than one state. For example, water can exist as a solid (ice), liquid, or gas (water vapor). The state of water depends on its temperature. Below 0°C, water is a solid. As the temperature rises above 0°C, ice melts to liquid water. When the temperature rises above 100°C, liquid water vaporizes completely. Some substances can exist in states other than solid, liquid, and vapor. For example, cholesterol myristate (a derivative of cholesterol) is a crystalline solid below 71°C. When the solid is warmed to 71°C, it turns into a cloudy liquid. When the cloudy liquid is heated to 86°C, it becomes a clear liquid. Cholesterol myristate changes from the solid state to an intermediate state (cloudy liquid) at 71°C, and from the intermediate state to the liquid state at 86°C. Because the intermediate state exits between the crystalline solid state and the liquid state, it has been called the liquid crystal state.

Liquid crystals are materials which has properties intermediate to the solid and liquid states of matters. They are true fluids (i.e. they flow readily), but they retain orientational order from solid to liquid crystal state .This is shown schematically in fig.1.1 where solid in the form of hexagonal crystal lattice melts to form liquid crystalline form before finally melting to normal liquid state

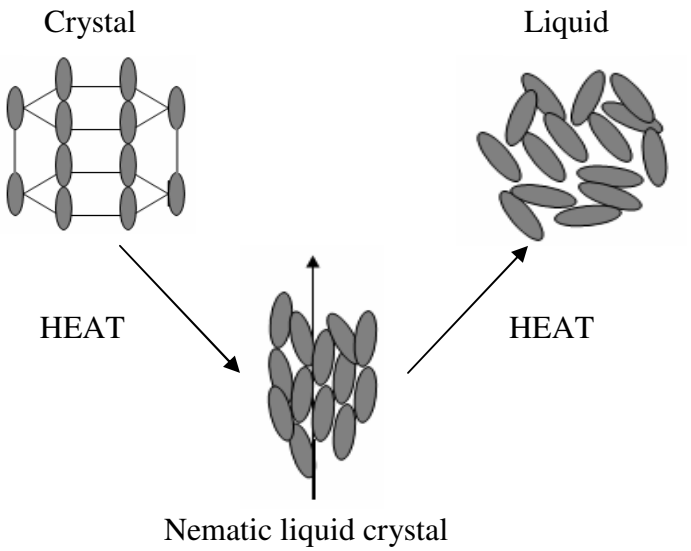

Fig. 1.1 On heating a crystal structure the molecules can form a oriented liquid crystal before becoming totally disordered in high temperature liquid crystal phase.

One of the prerequisites for a material to form liquid crystalline state is that the molecules are geometrically anisotropic. Put more simply, they must be different in different directions (i.e. cigar type). A spherical molecule cannot form a liquid crystal state as there is no preferred orientation which it can adopt. Liquid crystal materials generally have several common characteristics. Among these are

- a rod-like molecular structure
- rigidness of the long axis
- and strong dipoles and/or easily polarizable substituents.

The distinguishing characteristic of the liquid crystalline state is the tendency of the molecules (mesogens) to point along a common axis, called the director. This is in contrast to molecules in the liquid phase, which have no intrinsic order. In the solid state, molecules are highly ordered and have little translational freedom. The characteristic orientational order of the liquid crystal state is between the traditional solid and liquid phases and this is the origin of the term mesogenic state, used synonymously with liquid crystal state. The molecules are held in fixed positions by intermolecular forces. As the

temperature of a substance increases, its molecules vibrate more vigorously. Eventually, these vibrations overcome the forces that hold the molecules in place, and the molecules start to move. In the liquid state, this motion overcomes the intermolecular forces that maintain a crystalline state, and the molecules move into random positions, without pattern in location or orientation.

To quantify just how much order is present in a material, an order parameter (S) is defined. Traditionally, the order parameter is given as follows-

$$S = (1/2)\langle 3\cos^2\theta - 1\rangle$$

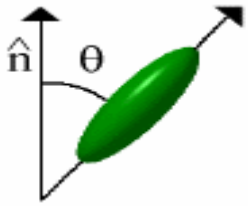

Fig. 1. Angle between the director and the long axis of each molecule.

Where θ, is the angle between the director and the long axis of each molecule. The brackets denote an average over all of the molecules in the sample. In an isotropic liquid, the average of the cosine terms is zero, and therefore the order parameter is equal to zero. For a perfect crystal, the order parameter evaluates to one. Typical values for the order parameter of a liquid crystal range between 0.3 and 0.9, with the exact value a function of temperature, as a result of kinetic molecular motion. This is illustrated below for a nematic liquid crystal material.

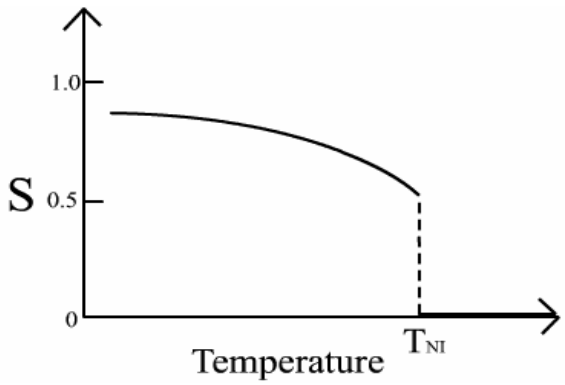

Fig. 1.3 Order parameter in liquid crystals

1.2.1.1 Characterizing Liquid Crystals

The following parameters describe the liquid crystalline structure:

- Positional Order
- Orientational Order
- Bond Orientational Order

Each of these parameters describes the extent to which the liquid crystal sample is ordered.

Most liquid crystal compounds exhibit polymorphism, or a condition where more than one phase is observed in the liquid crystalline state. The term mesophase is used to describe the "subphases" of liquid crystal materials. Mesophases are formed by changing the amount of order in the sample, either by imposing order in only one or two dimensions, or by allowing the molecules to have a degree of translational motion. The following section describes the mesophases of liquid crystals in greater detail.

1.2.1.2 Buliding blocks of liquid crystals

Substances that form liquid crystal structures are quite common. Approximately 0.5% of known carbon compounds have liquid crystal states. Liquid crystalline phase most often occur in compounds that have a shape that favor parallel packing like Rods (calamitic), Boards , disk/cones (discotic) [20]. Some examples are-

Rod like (calamitic):-

1. Methoxybenzilidene butylanaline (“MBBA”)

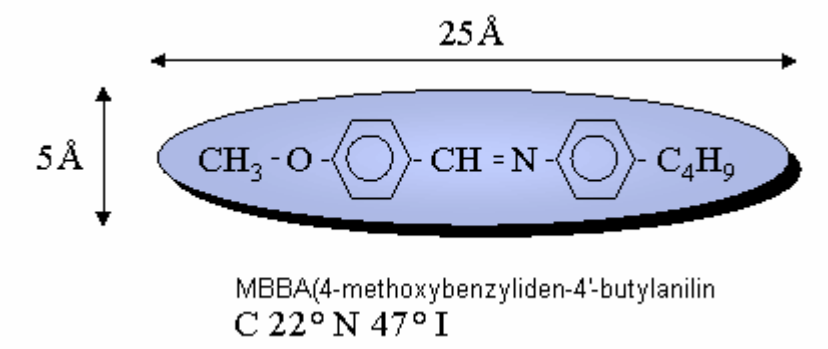

2. 4-Pentyl 4'-cynobiphenyl (5CB)

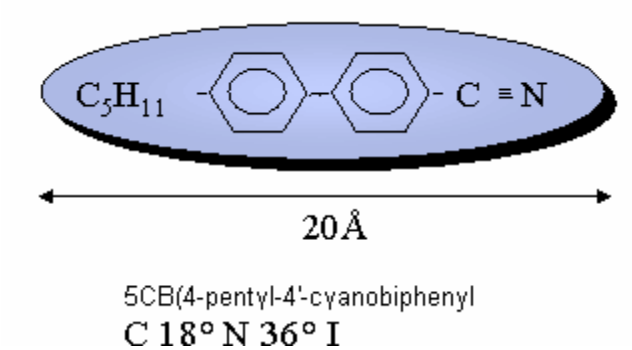

3. p-decyloxybenzlidene p'-amino 2-methylbutalcinnamate ("DOBAMBC")

Liquid cystals usually consist of steric "rod-" or "disk-like" organic molecules which tend to align themselves with a long range order due to anisotropic intermolecular forces.

1.2.1.3 Liquid Crystal Phases

The liquid crystal state is a distinct phase of matter observed between the crystalline (solid) and isotropic (liquid) states. There are many types of liquid crystal states, depending upon the amount of order in the material [20]. This section will explain the phase behavior of liquid crystal materials.

(a) Nematic Phases

The nematic liquid crystal phase is characterized by molecules that have no positional order but tend to point in the same direction (along the director). In the following diagram, notice that the molecules point vertically but are arranged with no particular order.

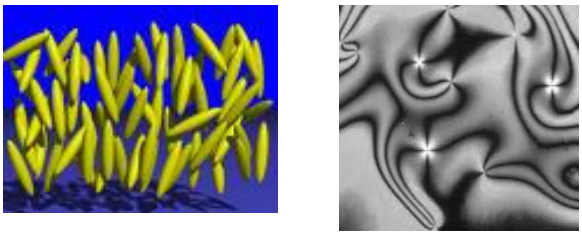

Fig. 1.4 (left) Picture of nematic phase, (right) Photo of nematic phase (using polarizing microscope)

Liquid crystals are anisotropic materials, and the physical properties of the system vary with the average alignment with the director. If the alignment is large, the material is very anisotropic. Similarly, if the alignment is small, the material is almost isotropic.

A special class of nematic liquid crystals is called chiral nematic. Chiral refers to the unique ability to selectively reflect one component of circularly polarized light. The term chiral nematic is used interchangeably with cholesteric.

(b) Smectic Phases

The word "smectic" is derived from the Greek word for soap. This seemingly ambiguous origin is explained by the fact that the thick, slippery substance often found at the bottom of a soap dish is actually a type of smectic liquid crystal.

The smectic state is another distinct mesophase of liquid crystal substances. In the smectic state, the molecules maintain the general orientational order of nematics, but also tend to align themselves in layers or planes. Motion is restricted to within these planes, and separate planes are observed to flow past each other. The increased order means that the smectic state is more "solid-like" than the nematic.

Fig. 1.5 Photo of a smectic phase (using polarizing microscope)

Many compounds are observed to form more than one type of smectic phase. As many as 12 of these variations have been identified, however only the most distinct phases are discussed here.

In the smectic-A mesophase, the director is perpendicular to the smectic plane, and there is no particular positional order in the layer. Similarly, the smectic-B mesophase orients with the director perpendicular to the smectic plane, but the molecules are arranged into a network of hexagons within the layer. In the smectic-C mesophase, molecules are

arranged as in the smectic-A mesophase, but the director is at a constant tilt angle measured normally to the smectic plane.

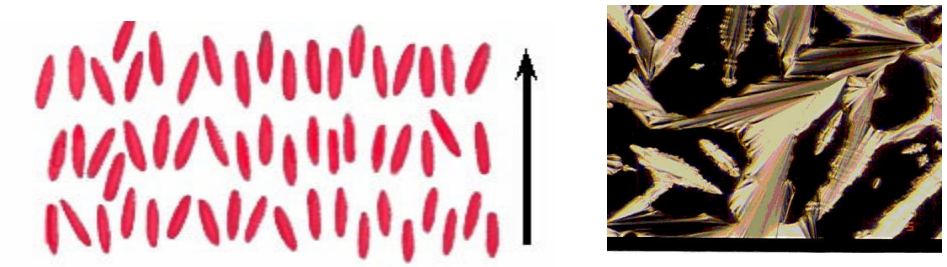

Fig.1.6 (left) Picture of the smectic A phase, (right) Photo of the smectic A phase (using polarizing microscope).

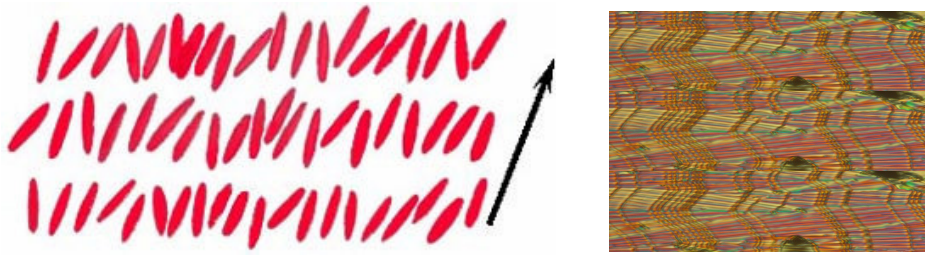

Fig1.7 (left) Picture of the smectic C phase, (right) Photo of the smectic C phase (using polarizing microscope)

As in the nematic, the smectic-C mesophase has a chiral state designated C*. Consistent with the smectic-C, the director makes a tilt angle with respect to the smectic layer. The difference is that this angle rotates from layer to layer forming a helix. In other words, the director of the smectic-C* mesophase is not parallel or perpendicular to the layers, and it rotates from one layer to the next. Notice the twist of the director, represented by the green arrows, in each layer in the following diagram (fig 1.8).

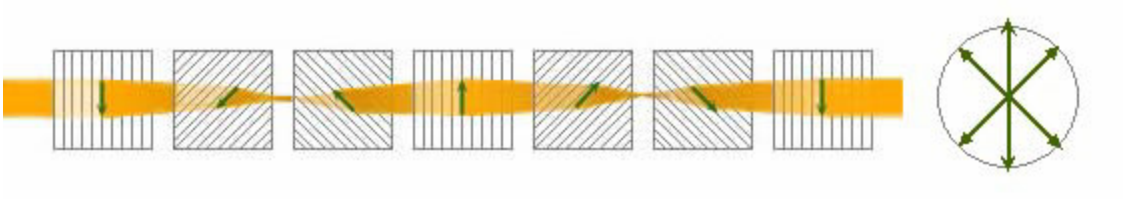

Fig.1.8 A schematic representation of a smectic C* phase (left), and a view of the same phase, but along the axis (right).

In some smectic mesophases, the molecules are affected by the various layers above and below them. Therefore, a small amount of three dimensional orders is observed. Smectic-G is an example demonstrating this type of arrangement.

The arrangement of the molecules within the columns and the structure of a molecule that forms the smectic C, smectic A, and nematic phases, and the temperatures at which each phase transition takes place is shown in the following fig.,

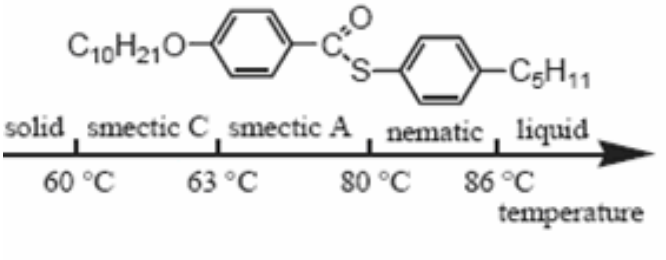

In order to gain some insight into the properties of these various liquid crystal phases, it is important to understand the concept of symmetry as it is applied to materials. The structure of a material is often such that, if the entire sample is translated in a certain direction by a specific distance, rotated about a specific axis by a certain angle, reflected through a plane oriented in a specific direction, or inverted through a specific point, then the structure of the material is unchanged. The nematic liquid crystal of Fig. 1.4 possesses all the possible symmetries of the liquid phase, except that the rotations about an axis perpendicular to the director are restricted to 180 if the structure is to remain unchanged. Thus the transition from the liquid phase to the nematic liquid crystal phase is one in which some rotational symmetry of the liquid phase is ‘‘broken.’’ Likewise, imagine the transition from the nematic liquid crystal phase to the smectic-A liquid

crystal phase. Whereas translations in any direction by any distance leave the nematic liquid crystal phase unchanged, translations along the director in the smectic-A liquid crystal phase are restricted to multiples of the layer spacing if the structure is to be unchanged. This restriction is another example of a symmetry broken at the transition from the nematic liquid crystal phase to the smectic-A liquid crystal phase. Symmetry considerations are important because all the properties of a substance must conform to the symmetry of the structure.

1.2.1.4 Electric and Magnetic Field Effects

The response of liquid crystal molecules to an electric field is the major characteristic utilized in industrial applications. The ability of the director to align along an external field is caused by the electric nature of the molecules. Permanent electric dipoles result when one end of a molecule has a net positive charge while the other end has a net negative charge. When an external electric field is applied to the liquid crystal, the dipole molecules tend to orient themselves along the direction of the field. In the following diagram, the black arrows represent the electric field vector.

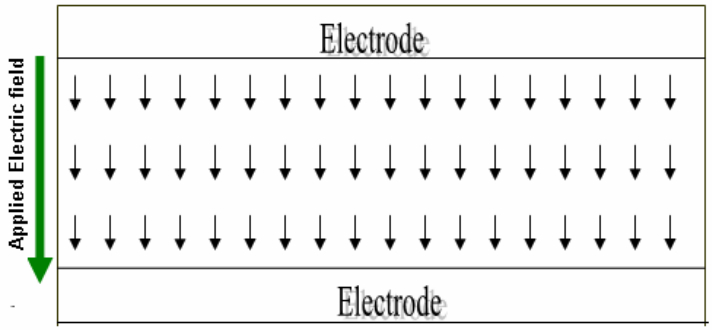

Fig. 1.9 Effect of external electric field on liquid crystals

Even if a molecule does not form a permanent dipole, it can still be influenced by an electric field. In some cases, the field produces slight re-arrangement of electrons and protons in molecules such that an induced electric dipole results. While not as strong as permanent dipoles, orientation with the external field still occurs.

The effects of magnetic fields on liquid crystal molecules are analogous to electric fields. Because magnetic fields are generated by moving electric charges, permanent magnetic

dipoles are produced by electrons moving about atoms. When a magnetic field is applied, the molecules will tend to align with or against the field.

1.2.1.5 Unique properties of Liquid Crystals

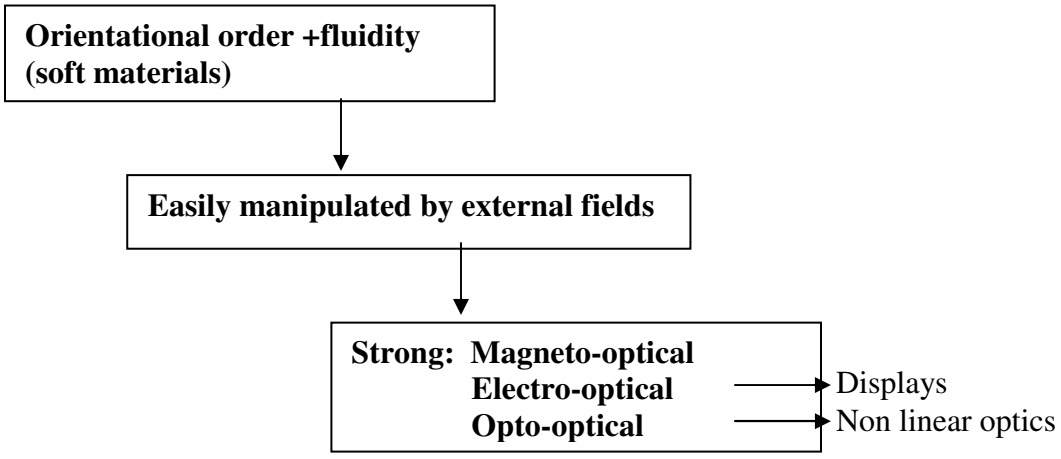

Fig. 1.10 Physical properties of liquid crystals

As a result of orientational order, most physical properties of liquid crystals are anisotropic and must be described by second rank tensors. Examples are the heat diffusion, the magnetic susceptibility, the dielectric permittivity or optical birefringence. Additionally, there are new physical qualities, which do not appear in simple liquids as e.g. elastic or frictional torques (rotational viscosity) acting on static or dynamic director deformations, respectively.

The most remarkable features of liquid crystals with respect to applications are due to their anisotropic optical properties. Nematics, and SmA are uniaxial, SmC weakly biaxial. Cholesterics give rise to Bragg reflections if the helix pitch is in the magnitude of the light wavelegth. As mentioned above these properties are carried by a fluid, soft material, and therefore are extremely sensitive against external perturbations.

Orientational order and hence birefringence can be manipulated easily e.g. with the help of rather weak magnetic, electric or optical fields, leading to huge magneto-optical, electro-optical and opto-optical effects. The most successful application are liquid crystal displays well-known from wrist watches, pocket calculators or flat screens of laptop

computer which take advantage of electro-optical effects. More recently, it turned out that orientational order can be also affected by optical fields leading to rather sensitive opto-optical effects and nonlinear optical properties, which are important e.g. for all-optical switching and other photonic devices in future optical information technologies.

1.2.2 What are Ferroelectric Liquid Crystals?

The Nematic and Smectic A (SA) liquid crystal phases are too symmetric to allow any vector order, such as ferroelectricity. The tilted smectics, however, do allow ferroelectricity if they are composed of chiral molecules. The pictures below show the original ferroelectric LC, DOBAMBC and a modern compound, W 314.

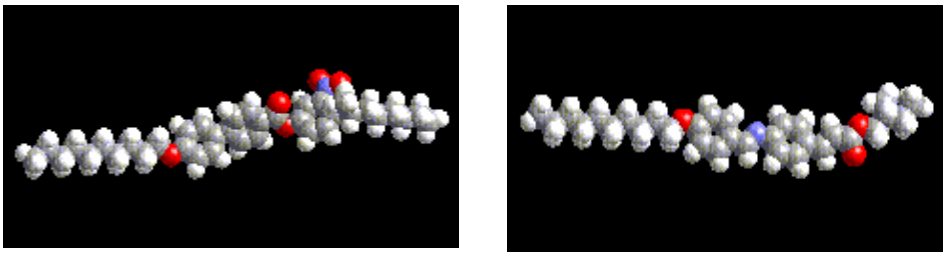

(a) (b)

Fig. 1.11 The pictures show the (a) original ferroelectric LC, DOBAMBC and (b) a modern compound, W 314.

In the simplest case, the Smectic C (SC), the average long molecular axis is tilted from the layer normal **z** by a fixed angle but the molecules are free to rotate on the so-defined tilt cone. The phase has a C_2 symmetry axis perpendicular to both the molecular director and the layer normal. The molecules exhibit a net spontaneous polarization along this axis. The magnitude of the polarization depends on temperature, generally decreasing as the tilt angle goes to zero at the SC - SA phase transition. The following Figure shows the geometry of the chiral Sm C phase:

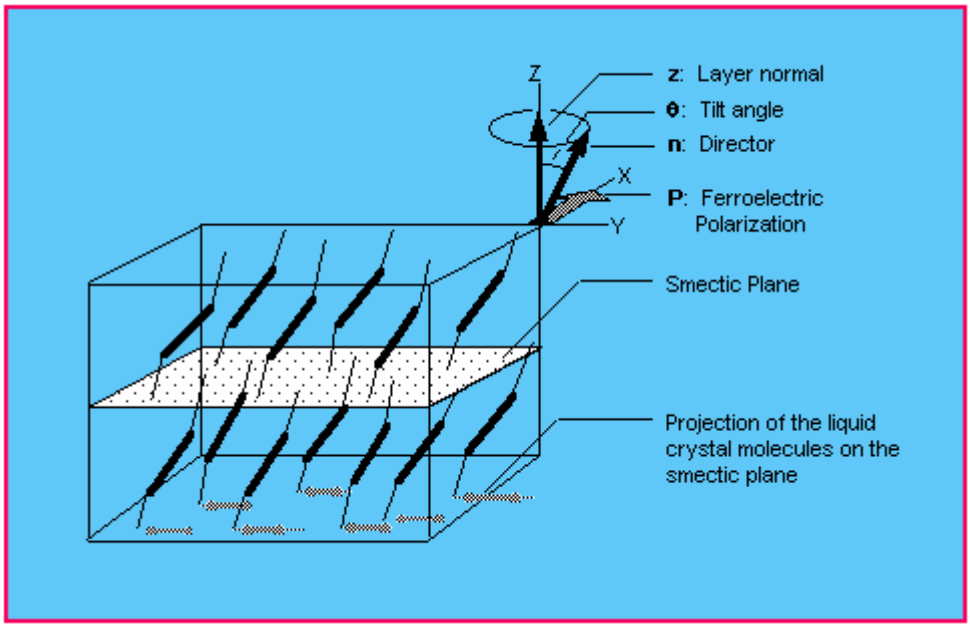

Fig. 1.12 The figure shows the geometry of the chiral Sm C phase.

Ferroelectric liquid crystals (FLCs) also exhibit a spontaneous helixing of the polarization, so that over macroscopic distances (a few microns, say) the polarization averages to zero.

As explained previously, the smectic-C liquid crystal phase possesses inversion symmetry and is therefore centrosymmetric. The situation changes dramatically, however, if the molecules are chiral. This is illustrated with the help of fig. 1.13, in which the molecules are depicted as fish with one black eye and one white eye. Such fish are chiral, in that inversion changes one kind into the other (just like the human hand). As demonstrated in Fig. 1.13, inversion seems to leave the structure unchanged until it is noticed that the fish that started out with one handedness have all been changed to fish of the other handedness. Inversion symmetry is not present and the structure is clearly non-centrosymmetric. An even closer look at fig. 1.15 reveals that the inverted structure has not been changed along the x- and z- axes, only along the y-axis. To see this, notice that if the eyes are ignored, the structure is unchanged. But the eyes lie along the y-axis, and they all have changed.

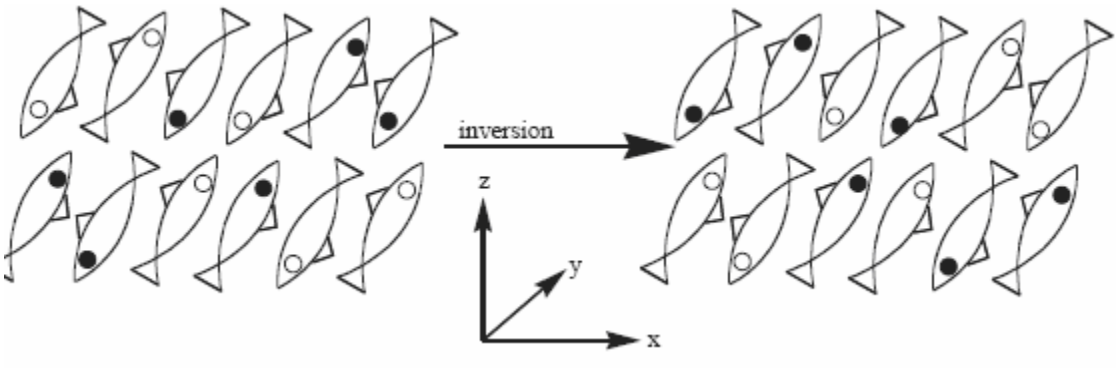

Fig. 1.13 Chiral Sematic C phase

Therefore, in a smectic liquid crystal phase of chiral molecules, the +y and -y directions are not equivalent. If the molecule possesses a non-zero electric dipole moment along the y-axis, then these will add together to produce a macroscopic electric polarization and a ferroelectric material. But theoretical speculation of this sort is hardly convincing without some proof that substances actually behave in this way. Although smectic-C liquid crystal phases had been studied prior to 1975, there were not many examples and none of them involved chiral molecules. Meyer's theoretical prediction of ferroelectric liquid crystals and experimental confirmation that they did indeed exist caught the interest and imagination of condensed matter scientists by storm. Here was an unanticipated area of material science, with new chemistry and physics just waiting to be discovered. The field of ferroelectric liquid crystals blossomed in no time, literally becoming the dominant area of study among the researchers studying liquid crystals. The list of newly synthesized ferroelectric liquid crystals is now over 50,000. Antiferroelectric liquid crystals and ferroelectric liquid crystals were subsequently discovered. Ferroelectric liquid crystals that spontaneously create defects brought to light an entirely different way that nature orders materials. The investigation of chiral liquid crystals also took on new life, as the power of Meyer's symmetry arguments led researchers to new phases, new kinds of phase transitions, and unforeseen properties.

1.2.3 Symmetry consideration of FLC

The X, Y, Z coordinate and the arrangement of the molecules in the SmC and SmC* phases are as shown:

SmC	SmC*
C_{2Y} $(P_X, P_Y, P_Z) \Rightarrow (-P_X, P_Y, -P_Z)$ $\Downarrow$ $P = (0, P_Y, 0)$	C_{2Y} $(P_X, P_Y, P_Z) \Rightarrow (-P_X, P_Y, P_Z)$ $\Downarrow$ $P = (0, P_Y, 0)$

In both the SmC (symmetry C_{2h}) and SmC* (symmetry C_2) phases, 180˚ rotation around the Y- axis is an allowed symmetry operation. In the SmC phase the XZ plane is a mirror plane.

Reflection in the XZ - Plane

SmC	SmC*
m_{xz} $(0, P_Y, 0) \Rightarrow (0, -P_Y, 0)$ $\Downarrow$ $P = (0, 0, 0)$ Ferroelectricity not allowed	**Reflection not allowed due to chirality** $\Downarrow$ $P = (0, P_Y, 0)$ Ferroelectricity allowed

Since these two expressions must be identical, p must be zero and ferroelectricity is not allowed in the SmC phase. In SmC* phase, the molecules are chiral and not any more mirror images of them selves. Thus the XZ- plane is not any longer a mirror plane and ferroelectricity is permitted by symmetry. The spontaneous polarization in the smectic C* phase points the direction along Y-axis. It lies in the smectic planes in a direction perpendicular to the tilt plane.

1.3 CARBON NANO TUBES- FERROELECTRIC LIQUID CRYSTAL COMPOSITE

Carbon nanotubes are the focus of intense research due to their unique physical properties, namely their anisotropic mechanical, thermal and electronic behavior. Single-walled nanotubes (SWNTs) show high conductivity along the tube length and very low conductivity across the tube diameter [21, 22]. SWNTs are also known to align parallel to each other in low concentration solutions while multi-walled nanotubes (MWNTs) show a propensity to spontaneously form lyotropic liquid crystalline phases above a critical CNT concentration [23,24,25]. The inherent conductivity and spontaneous selfalignment properties of CNTs make them an attractive alternative as an alignment layer. The

anisotropy of the electric conductivity, being large (metallic or semiconductor) along the tube axis and small perpendicular to it, has led to proposals of nanotubes being used as molecular wires in nano-scale electronics and transistor, or as field emission sources. Other possible applications include their use as actuator or nano-sensor for chemical and biological molecular direction.

1.4 WHAT ARE NANO TUBES?

A nanotube is a cylinder made up of atomic particles and whose diameter is around one to a few billionths of a meter. They can be made from a variety of materials.

Nanotubes vary by the number of cylinders; there are nanotubes made up of a single cylindrical layer but there are also reinforced nanotubes comprised of two or more cylindrical layers (one nanotube cylinder completely encloses another). Wall thickness also differs; some nanotubes are thicker than others. Since nanotubes vary by wall thickness and number of cylinders, the radius of nanotubes is also variable. Moreover, the length of nanotubes is also not universal. Finally, nanotubes can be organic or inorganic, depending on the particles used in nanotube construction.

A **nanotube** is a nanometer scale wire-like structure that is most often composed of carbon. But inorganic nanotubes have also been synthesised, including:

- boron nitride
- silicon
- titanium dioxide (B)
- tungsten disulphide
- molybdenum disulphide

1.4.1 Carbon Nanotubes

Carbon nanotubes (CNT) are tiny cylindrical carbon structures with a diameter in the range of nanometers (10-9 meters). Structure of a nanotube consists of one cylinder or more coaxial cylinders of graphene sheet placed between two halves of a fullerene molecule (buckyball).

Certainly we knew the two types of naturally occuring all-carbon allotropes with crystalline structure-

- covalent bonded diamond
- graphite (hexagonal structure)

Nanotubes are fundamental new structures, containing carbon atoms. The breakthrough in carbon science came from experiments on clusters formed by laser vaporisation of graphite, which finally yields to the discovery of Carbon Nanotubes by Iijima in the NEC-laboratories (Japan, 1991) by inspecting the cathodes after graphite arc vaporisation.

Carbon nanotubes (CNTs) are allotropes of carbon. A single wall carbon nanotube is a one-atom thick sheet of graphite (called graphene) rolled up into a seamless cylinder with diameter of the order of a nanometer. This results in a nanostructure where the length-to-diameter ratio exceeds 10,000. Such cylindrical carbon molecules have novel properties that make them potentially useful in a wide variety of applications in nanotechnology, electronics, optics and other fields of materials science. They exhibit extraordinary strength and unique electrical properties, and are efficient conductors of heat. Inorganic nanotubes have also been synthesized.

Nanotubes are members of the fullerene structural family, which also includes buckyballs. Whereas buckyballs are spherical in shape, a nanotube is cylindrical, with at least one end typically capped with a hemisphere of the buckyball structure. Their name is derived from their size, since the diameter of a nanotube is on the order of a few nanometers (approximately 50,000 times smaller than the width of a human hair), while they can be up to several millimeters in length. There are two main types of nanotubes: single-walled nanotubes (SWNTs) and multi-walled nanotubes (MWNTs).

1.4.1.1 Single-walled nanotubes

Most single-walled nanotubes (SWNT) have a diameter of close to 1 nanometer, with a tube length that can be many thousands of times longer. The structure of a SWNT can be

conceptualized by wrapping a one-atom-thick layer of graphite called graphene into a seamless cylinder. The way the graphene sheet is wrapped is represented by a pair of indices (n,m) called the chiral vector. The integers n and m denote the number of unit vectors along two directions in the honeycomb crystal lattice of graphene. If m=0, the nanotubes are called "zigzag". If n=m, the nanotubes are called "armchair". The terms "armchair" and "zig-zag" refer to the arrangement of hexagons around the circumference otherwise, they are called "chiral", meaning that it can exist in two mirror-related forms as shown in figure 1.14.

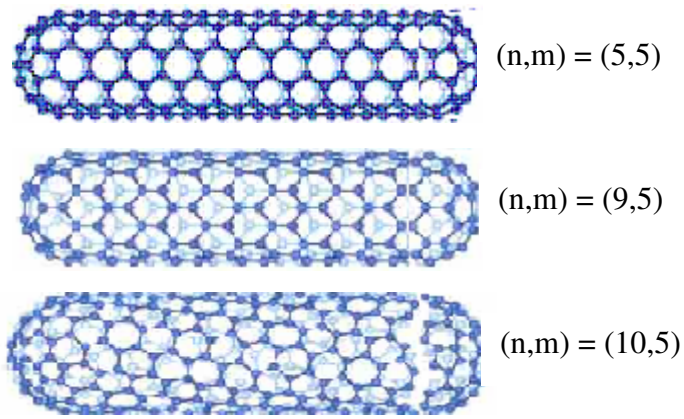

Fig. 1.14 The first two of these, known as “armchair” (top) and “zig-zag” (middle) have a high degree of symmetry. The third class of nanotube is known as chiral (bottom).

Single-walled nanotubes are a very important variety of carbon nanotube because they exhibit important electric properties that are not shared by the multi-walled carbon nanotube (MWNT) variants. Single-walled nanotubes are the most likely candidate for miniaturizing electronics past the micro electromechanical scale that is currently the basis of modern electronics. The most basic building block of these systems is the electric wire, and SWNTs can be excellent conductors [26]. One useful application of SWNTs is in the development of the first intramolecular field effect transistors (FETs).

1.4.1.2 Multi-Walled Nanotubes

Multi-walled nanotubes (MWNT) consist of multiple layers of graphite rolled in on themselves to form a tube shape. There are two models which can be used to describe the structures of multi-walled nanotubes. In the Russian Doll model, sheets of graphite are arranged in concentric cylinders, e.g. a (0, 8) single-walled nanotube (SWNT) within a larger (0,10) single-walled nanotube as shown in figure 1.15. In the Parchment model, a single sheet of graphite is rolled in around itself, resembling a scroll of parchment or a rolled up newspaper. The interlayer distance in multi-walled nanotubes is close to the distance between graphene layers in graphite, approximately 3.3 Å. The special place of double-walled Carbon Nanotubes (DWNT) must be emphasized here because they combine very similar morphology and properties as compared to SWNT, while improving significantly their resistance to chemicals.

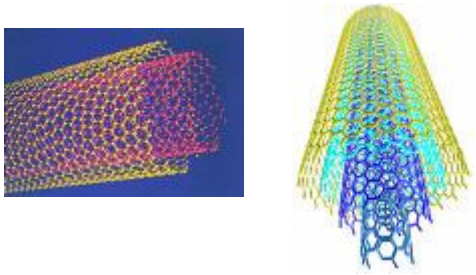

Fig. 1.15 Typical structures of multiwalled nanotubes.

1.4.2 Why MWNTs are preferred?

1. MWNTs are less expensive than SWNT.
2. MWNTs are more chemical resistant than SMNT. This is especially important when fictionalization is required (this means grafting of chemical functions at the surface of the nanotubes) to add new properties to the CNT. In the case of SWNT, covalent fictionalization will break some C=C double bonds, leaving "holes" in the structure on the nanotube and thus modifying both its mechanical and electrical properties. In the case of DWNT, only the outer wall is modified.

1.4.3 Properties of Carbon Nanotubes

The strength of the sp^2 carbon-carbon bonds gives carbon nanotubes amazing mechanical properties. The stiffness of a material is measured in terms of its Young's modulus, the rate of change of stress with applied strain. The Young's modulus of the best nanotubes can be as high as 1000 GPa which is approximately 5x higher than steel. The tensile strength, or breaking strain of nanotubes can be up to 63 GPa, around 50x higher than steel. These properties, coupled with the lightness of carbon nanotubes, give them great potential in applications such as aerospace. It has even been suggested that nanotubes could be used in the "space elevator", an Earth-to-space cable first proposed by Arthur C. Clarke. The electronic properties of carbon nanotubes are also extraordinary. Especially notable is the fact that nanotubes can be metallic or semiconducting depending on their structure. Thus, some nanotubes have conductivities higher than that of copper, while others behave more like silicon. There is great interest in the possibility of constructing nanoscale electronic devices from nanotubes, and some progress is being made in this area. However, in order to construct a useful device we would need to arrange many thousands of nanotubes in a defined pattern, and we do not yet have the degree of control necessary to achieve this.

Most important application of Carbon Nanotubes is in LCDs as Carbon nanotubes have high aspect ratio i.e. length to thickness ratio. Carbon Nanotubes give the better alignment (selfalignment) to the liquid crystal molecules and hence increases the properties of Liquid crystals i.e. dielectric properties, switching response and their morphological properties.

1.5 AIM OF THE THESIS

In the frame of this thesis, insights into the fundamental problems in the fabrication of CNT- based composite are presented. We find that embedding the carbon nanotubes in a LC results in changes of the dielectric spectra of the matrix, caused by the strong interaction between LC and carbon nanotubes. Thus in our thesis we will concentrate on the influence of carbon nanotubes on the dielectric and morphological properties of FLC.

CHAPTER 2
Experimental techniques

2.1 REVIEW

In the past more then three decades, material scientists have been exploring novel materials for applications in various electro-optical control and display devices such as optical shutters, switchable privacy windows, and reflective color displays. Ferroelectric liquid crystal (FLC) and nanotube (NT) dispersed ferroelectric liquid crystal (NTDFLC) is a class of materials, normally prepared by ultrasonification of an initially homogeneous solution of liquid crystal (LC) and nanotubes. Therefore the selection of materials plays an important role on the performance of NTDFLC devices. The selections of materials in the present study has been made on the basis of their physical properties e.g. homogeneous mixing of NTs and liquid crystal, dispensability of NTs in liquid crystals, their purity, and the most important is the nanotubes concentration in NTDFLC devices. For the preparation of CNT dispersed ferroelectric liquid crystal films by ultrasonification method, several factors, i.e. time duration of ultrasonification, concentrations of liquid crystal, concentration of CNTs and the size of the spacer, were adjusted.

Carbon nanotubes (CNTs) as homogeneous materials found a wide practical application. Their composites with other materials, in particular, with liquid crystals (LCs), are of growing interest from scientific and technological points of view. A number of publications appeared recently in which properties of the CNTs dissolved in LCs and properties of CNTs film–LC interfaces were studied. Previous studies showed that the CNTs are difficult to dissolve in LCs. They cannot form stable solutions, since solid CNTs easily aggregate even at small concentrations in LC. In the present work, we report on the formation of CNTs–LC systems stable in time. Frequency dependence of complex dielectric permittivity was studied to analyze how the properties of each component of the composite can influence dielectric parameters of the whole system.

2.2 MATERIALS

In the present work, the liquid crystal mixture and liquid crystals used in our experiments were commercially available ferroelectric liquid crystal mixture namely ZLI 4237-100, which has comparatively large dielectric anisotropy, and large temperature range over which the sematic phase exists. The nanotubes used in the experiments were carbon nanotubes with dimensions 110-170 nm, length between 5-9 micron and purity of 90+ %. Transition temperatures in Celsius are also provided in the figures, where Cryst, SmC, SmA, N* stand for crystalline phase, smectic C phase, smectic A phase, and chiral nematic phase, respectively.

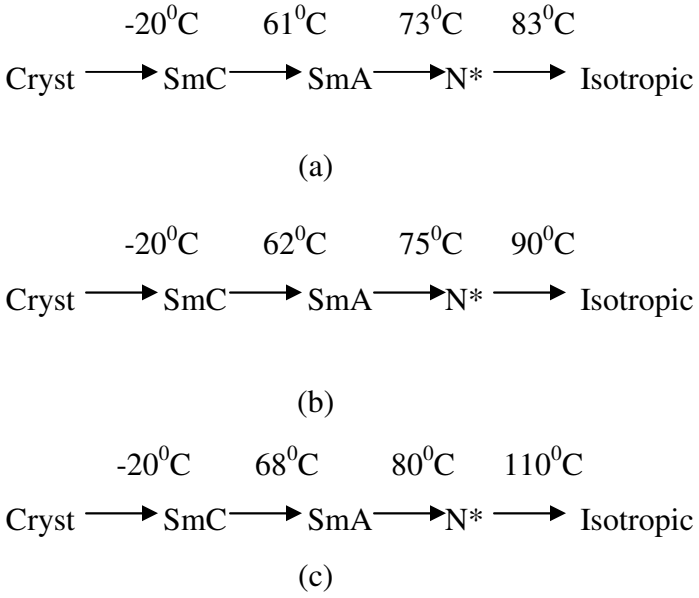

Fig. 2.1 Phase sequence of liquid crystal (a) neat FLC (b) 0.05% CNTs dispersed FLC (c) 0.1% CNTs dispersed FLC

2.3 PREPARATION OF SAMPLE CELLS

Ferroelectric liquid crystal (LC) and carbon nanotubes dispersed liquid crystal (CNTDLC) sample cells were prepared using conducting indium tin oxide (ITO) coated glass substrates. Glass substrates were procured from Bharat Electronics Limited (BEL), Bangalore. Some commercial cells obtained from M/S Linkam Instruments, UK were also used in the experiment. These ITO coated glass substrates were highly transparent

with resistivity of the order of few 140-180 ohm-m. The substrates were initially washed with soap solution, rinsed with acetone (purity 99.9%), distilled water and then dried in a vacuum chamber. These substrates were then put in dust free (laminar flow) chamber to ensure proper cleaning conditions.

The characterization with respect to morphological and dielectric studies etc was carried out in aligned and unaligned sample cells. Out of the two basic forms of alignment for liquid crystalline compounds or mixtures i.e. the homeotropic and homogenous [28-32], we used homogenous alignment method. In this method constituents molecules of LC phase are oriented parallel to the supporting substrates. The conducting sides of these ITO coated glass substrates were joined together and separation between the substrates was maintained with the help of mylar spacer of different thickness (µm). These two glass plates were sealed with optical adhesive (UV curable polymer), and then cured the cell in presence of UV light. The electrodes were connected at the ITO coated substrate surface of the cell using indium (metal) ingot to obtaining better contact.

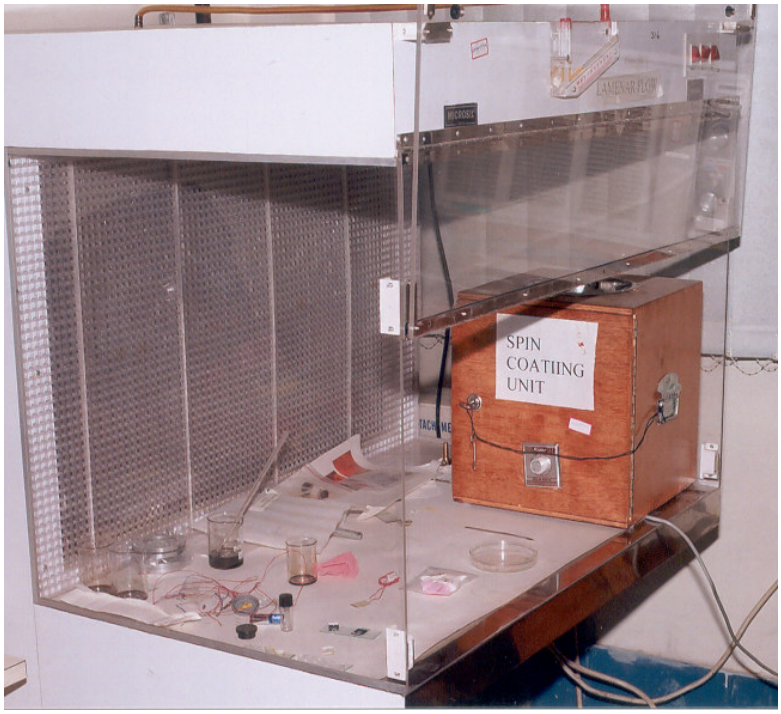

Fig. 2.2 Dust free (laminar flow) chamber for liquid crystal cell preparation.

2.4 Preparation of CNTs dispersed ferroelectric liquid crystal samples

One of the most challenging tasks is to disperse the CNTs, which has a tendency for aggregation. These CNTs aggregates generally form micrometer scale agglomerates that can be seen under optical microscopy. Mechanical agitation was necessary to disrupt the large agglomerates, but it is evidently insufficient to disperse the CNTs on a finer scale. To achieve a finer dispersion of CNTs, sonication was applied to the CNT mixture, although molecular level dispersion was hard to realize. We employed a mixing of CNTs in ferroelectric liquid crystal (FLC) at ambient temperature. To ensure completing dispersing of CNTs in ferroelectric liquid crystal, few drops of chloroform is added and ultrasonification is done at 42 kHz and 60^0 C. The cell gaps were maintained with mylor spacer between the substrates in all the samples. The same methodology was applied to the mixture of different concentration of CNTs in order to make a valid comparison with the results from the CNT-FLC mixture. The mixture was then sandwiched in between indium tin oxide (ITO) coated glass substrates by capillary action, giving a sample thickness of 5 μm. The sample cells were sealed by optical adhesive and then cured under UV light (intensity ~ 2 mW/cm^2) for about an hour at room temperature. The complete methodology of samples preparation is shown in Fig. 2.3 in the form of flow chart. An assembly of liquid crystal cell in empty and filled state is shown in Fig. 2.4

After sealing and curing, the samples were placed in a LINKAM temperature programmer cum hot-stage. The optical micro-texture and nanotubes dispersion were viewed at a magnification of 100X and 500X through Olympus polarizing microscope fitted with charge coupling device (CCD) camera. The CNTDLC morphology, its dispersion was detected and acquired on a P IV computer using Linksys and RTVMS software. The electric field was applied using a function generator and the output responses were detected on a digital storage oscilloscope using wavestar software. The detailed investigation on CNTs dispersed FLC, dielectric permittivity, dielectric loss, etc as a function of temperature, electric filed, CNTs concentrations etc are given in the chapter 3.

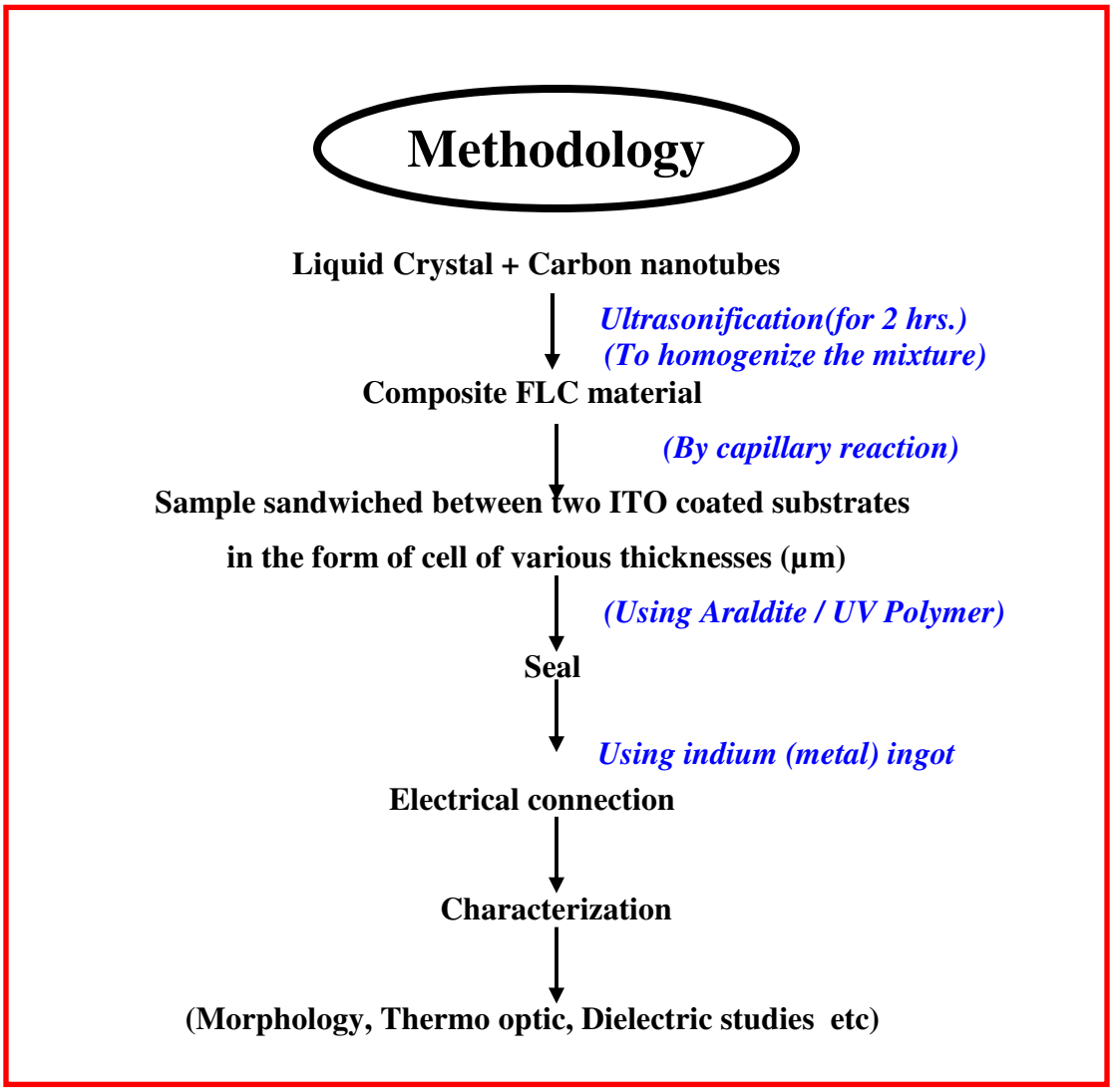

Fig. 2.3 A flow chart for the preparation of CNTs dispersed ferroelectric liquid crystal samples.

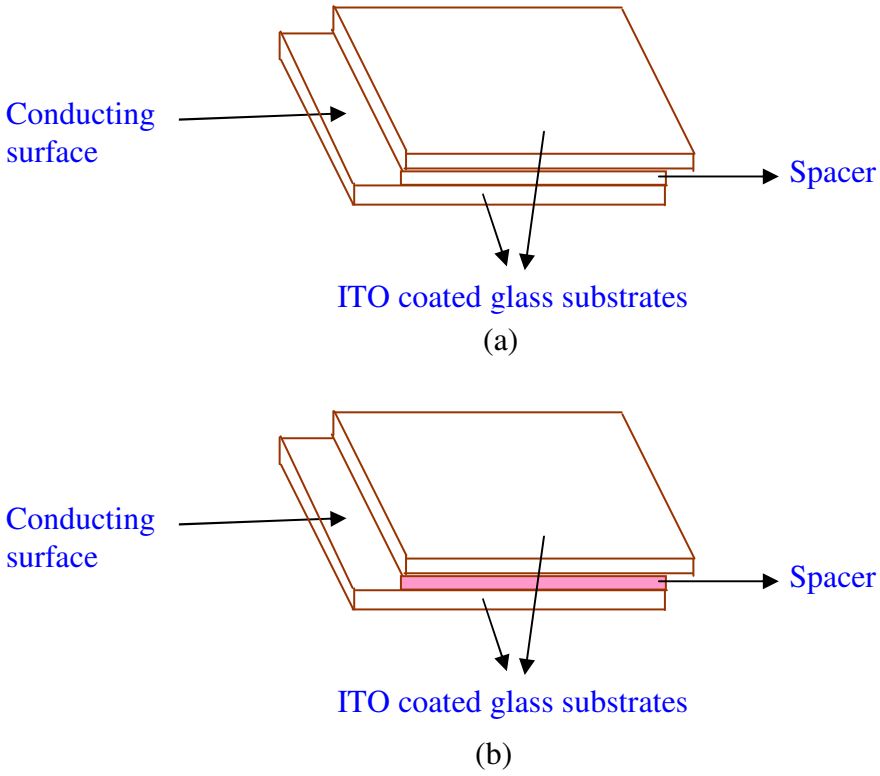

Fig. 2.4 An assembled (a) empty (b) filled liquid crystal cells

2.5 Provisional techniques

In order to study the liquid crystal morphology and phase transition temperatures, Olympus polarizing microscope (Model- BX51P) and Linkam temperature programmer cum hot stage (Model TP94 and THMS 600) were used. The electric field was applied to the sample through Scientech function generator (Model ST 4060), Philips function generator (Model FG8002). The microscopic optical textures were captured through the charge coupling device (CCD) digital camera (Olympus DP 12 JAPAN) fitted on polarizing microscope and interfaced to a computer. A block diagram of our experimental set-up for the investigation of optical textures, electro-optic properties and other parameters of liquid crystal is shown in Fig. 2.5 The temperature of the CNTDFLC sample cell was controlled using temperature controller interfaced with computer through RS232 port and the output response as a function of field was recorded on a Tektronix Oscilloscope (Model TDS2024). Uniform dispersion of Carbon nanotubes in the FLC and

all the optical textures were viewed under crossed polarizers at a total magnification of 100X and 500X in the transmission mode. The complete experimental set-up to study morphological properties is also shown in Fig. 2.6.

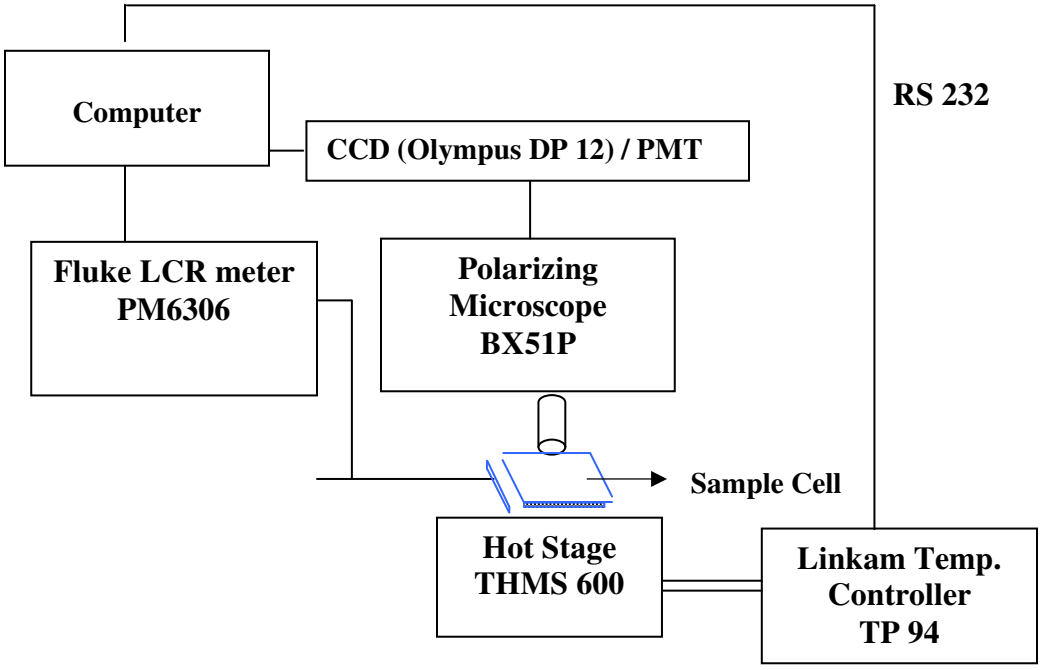

Fig. 2.5 Block diagram of the experimental set-up to study electro-optical properties.

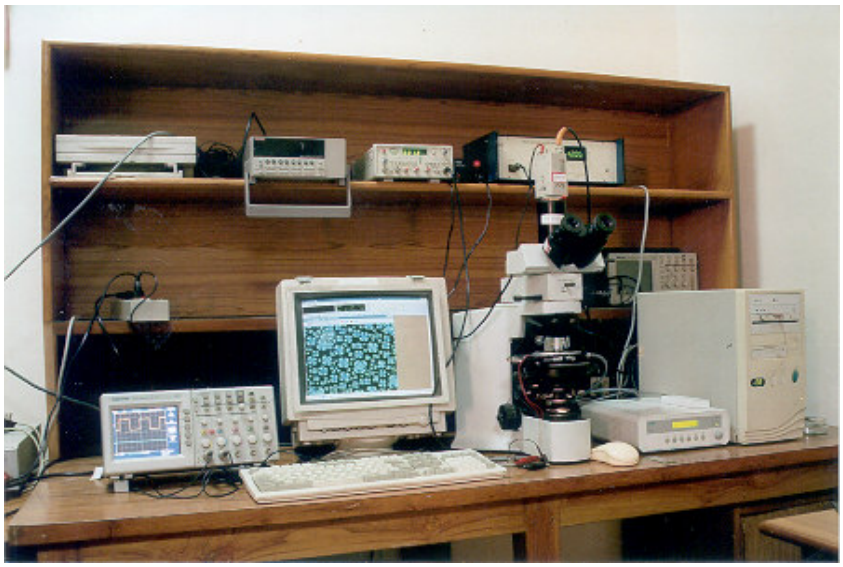

Fig. 2.6 Experimental set-up in the lab to study the morphological and dielectric studies of CNTDLC films

2.5.1 Optical polarizing microscopy

The optical studies observed in ferroelectric liquid crystal and CNTs dispersed ferroelectric liquid crystals investigated using an Olympus optical polarizing microscope (Model BX51P) at a magnification of 100X under crossed polarizers using long working distance objective lens. The optical micro-textures of LC materials were also investigated as a function of temperature, voltage and other physical parameters.

2.5.2 Temperature programmer along with hot stage

In thermal microscopy studies, we used Linkam temperature programmer TP94 and hot stage THMS 600. The TP94 is specifically designed for precise temperature control of the Linkam heating/freezing stages. The stage sensor is digitally linearized to give accurate temperature readout, the controls and their functions have been carefully chosen for simple and easy operation. The temperature range is –196 ^{o}C to 600 ^{o}C. Heating or cooling rates can be changed almost instantly using the three rate keys. The heat ranges are from 0.1 to 0.9^{o}C/min at 0.1 degree intervals from 1.0 to 9.0 ^{o}C/min at 1.0 degree intervals and from 10 to 90^{o}C degree intervals. A varying dc signal is used to control the stage and results in an even application of power, which avoids the bursts seen with conventional burst fire ac techniques. An optional remote control gives single key control of three programmable heating/cooling rates and the HEAT, COOL and HOLD functions. The three programmable heating/cooling rates are held in memory when power is switched off. The temperature and limit values can also be stored and recalled using the remote control facility.

2.5.3 Differential scanning calorimetry (DSC)

Differential scanning calorimetry (DSC) is a thermal analysis technique that measurers heat flow to and from a specimen as a function of time and temperature. DSC is one of the most widely used analytical instrument because of the ease with which it can provide large amount of thermodynamic data. Properly used, information on the phase transitions of a sample, such as transition temperature, enthalpy, heat capacity, specific heat, can all be calculated from a single data run. Enthalpy, a term often used in physical chemistry, is a measure of the chemistry, is a measure of the energy of the system that includes the

energy due to the volume that the system occupies. This experiment was an attempt to use DSC to examine the phase transitions and thermodynamic properties of the liquid crystal ZLI 4237-100 containing different concentration of carbon nanotubes. The phase transition temperature of the materials, noted through thermal polarizing microscopy was fully supported by differential scanning calorimetry. The DSC (Lineseis DSC L 63) used in the experiment was controlled by a compatible computer running the LINESEIS DSC instrumental software. The software collected data and provided graphical analysis tools to determine transition temperatures and peak areas. The DSC (Lineseis DSC L 63) used in the experiment is shown in the Fig. 2.7.

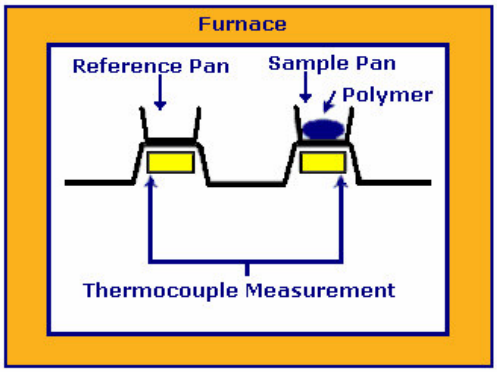

Fig. 2.7 Experimental setup for DSC

2.5.5 Dielectric measurements

The dielectric measurements were carried out using a programmable automatic RCL meter (FLUKE PM 6306) in the frequency range 50Hz to 1MHz. The cell was calibrated using air and benzene as standard references. The frequency and bias dependence of the real and imaginary parts of the complex dielectric permittivity have been studied in detailed at room temperature. The dielectric properties of the CNTDFLC were made in the presence of applied voltages that produced alignment (and, therefore, optical switching) of the LC phase. Dipole relaxation and ion-conduction-related processes were observed for samples. The dielectric behavior gave information on the reorientational motions of dipoles and the conduction behavior of extrinsic ions in the samples.

Fig. 2.8 Programmable automatic RCL meter [FLUKE PM6306] used for dielectric studies.

CHAPTER 3
Results and discussions

A consistent growth (both theoretical and experimental) has been seen in the subject of ferroelectric liquid crystal (FLC) materials soon after their discovery by Meyer et al. in 1975. Dielectric spectroscopy of a number of FLC has been investigated and possible information about their molecular orientation and the relaxation process explained in detail [33-41]. It is due to the fact that these materials are very interesting and promising for practical applications [42, 43]

The dielectric measurements of chiral smectic C (SmC*) [FLC] and CNTs dispersed in SmC* gives useful information about the static and the dynamic properties of these compounds. The ferroelectric SmC* phases is the consequence of a spatially modulated structure.

Morphological and dielectric studies have been carried out in a novel FLC mixture [FLC] whose phase sequence is given by

$$\text{Cryst} \xrightarrow{-20^0\text{C}} \text{SmC} \xrightarrow{61^0\text{C}} \text{SmA} \xrightarrow{73^0\text{C}} \text{N*} \xrightarrow{83^0\text{C}} \text{Isotropic}$$

3.1 Morphological studies of CNT dispersed FLC

Fig. 3.1(a) shows optical micrographs exhibiting large CNTs aggregates in the continuum of FLC prepared by simply shaking the compound. Mechanical agitation was necessary to disintegrate such large agglomerates, but it alone was inadequate to achieve finer dispersion. We therefore employed sonification of the CNT-FLC mixtures for about 2 hours. At 90^0C, well above the Smectic C* – isotropic transition temperature, the sample appeared optically clear to the naked eye, suggestive of a finer dispersion of CNT as shown in Fig.3.1 (b).

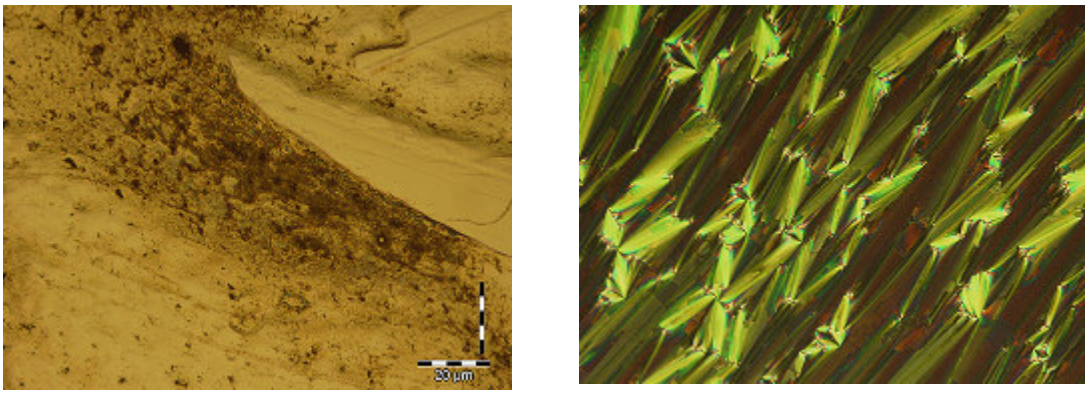

(a) (b)

Fig.3.1 Optical micrographs of 0.1% MWCNT in FLC (a) with shaking (b) after sonification

The concentration of the CNT-FLC mixtures was diluted by decreasing the concentration of CNTs and the diluted procedure was repeated to achieve very dilute solutions down to about 0.05%wt/wt.

Fig 3.2 shows micrographs of a 0.1% CNT concentration obtained under crossed polarizer at an elevated temperature appreciably above the smectic– isotropic transition temperature (T_{SI}) in FLC. The micro texture at 110^0C was dark under crosses polarizer, suggesting that the CNT-FLC mixture is in the isotropic state. To our surprise, birefringent domain structures appear at 103^0 C, which is significantly higher than the transition temperature from N* phase to isotropic phase of neat FLC. The structure continues to grow at the expense of the smaller domains (see the picture at 99^0C). The structure further evolves to larger chiral nematic domains with showing disclinations line (95 ºC). The growing chiral nematic domains eventually coalesce at 78^0C and the interface disappears, exhibiting Smectic A phase at ambient temperature. Our textural study confirms that the Smectic A – Smectic C* transition temperature of the mixed CNT-FLC is located about 68 ºC. This enhanced T_{NI} in the CNT-FLC mixture may be attributed to the anisotropic alignment of FLC induced by the CNT bundles. The entropy loss due to the mutual alignment of FLC and CNTs may be counterbalanced by enhanced interaction between the constituents; because the parallel alignment between the nanotube and liquid crystal molecules will increase the number of intermolecular contacts relative

to the centre-of-mass to centre-of mass interaction in the case of random orientation. A similar enhanced behavior of transition temperature from N* to isotropic phase can be confirmed in the 0.05% CNTs concentration. On decreasing to, 0.05%, the transition temperature of N* to isotropic is decreased to 90 ^{0}C. This transition eventually approaches to that of the FLC with further decrease of the nanotube concentration and then declines further to 83 ^{0}C at 0% CNT (FLCs).

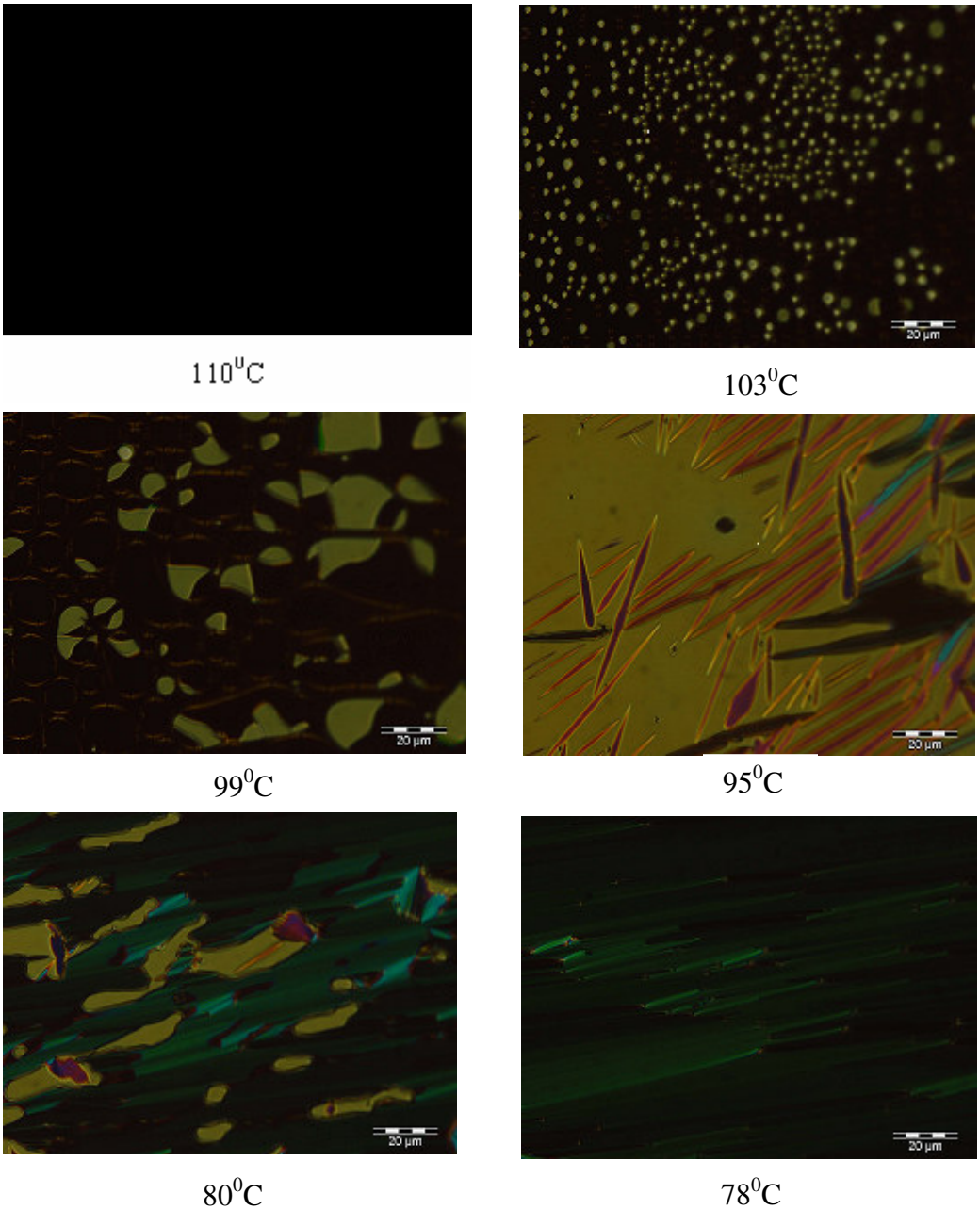

Fig. 3.2 Micrographs showing structural evolution during cooling from the isotropic (110^{0}C) to ambient temperature.

It is important to confirm the above observation of enhanced transition temperature in the CNT- FLC composites by other independent methods like thermo graphy (DSC). Fig 3.3 shows DSC profiles of FLC and its mixtures containing 0.1% and 0.05% wt/wt CNT. When the CNT content increased slowly from 0 to 0.05%, there was little enhancement (6–7^{0}C) in T_{NI} of the liquid crystal component. However, a pronounced enhancement of T_{NI} was observed for a very narrow range (0.05–0.1%) of Figure 3.3. DSC thermograms of CNT-FLC mixtures, containing 0.1% CNTs, 0.05% CNTs, FLC are shown in Fig 3.3. When the CNT concentration falls below 0.1%, to 0.05%, the T_{NI} transition peak drops back to 90^{0}C, and continues to decline gradually with further reduction of CNT concentration.

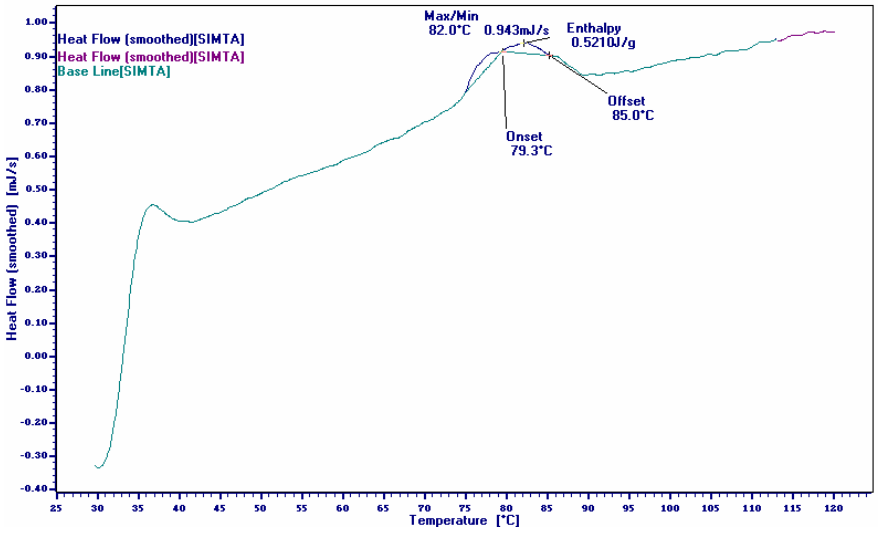

(a)

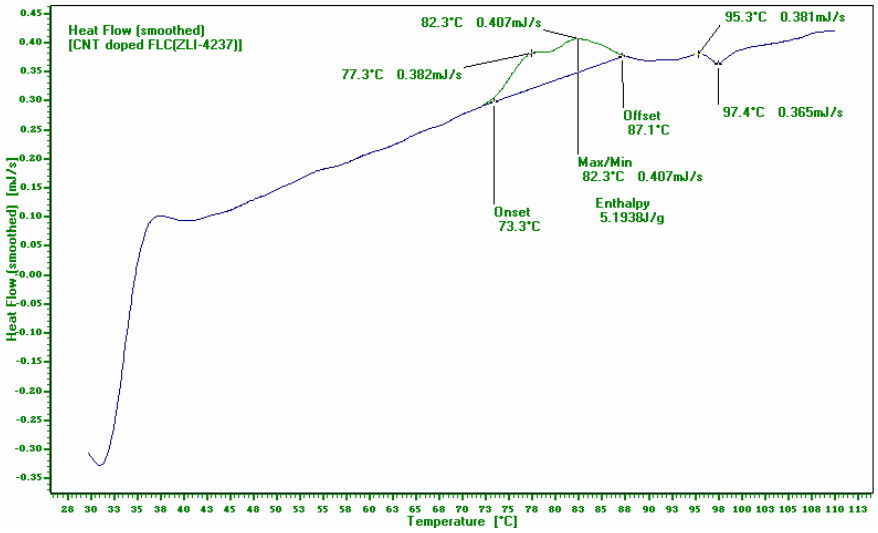

(b)

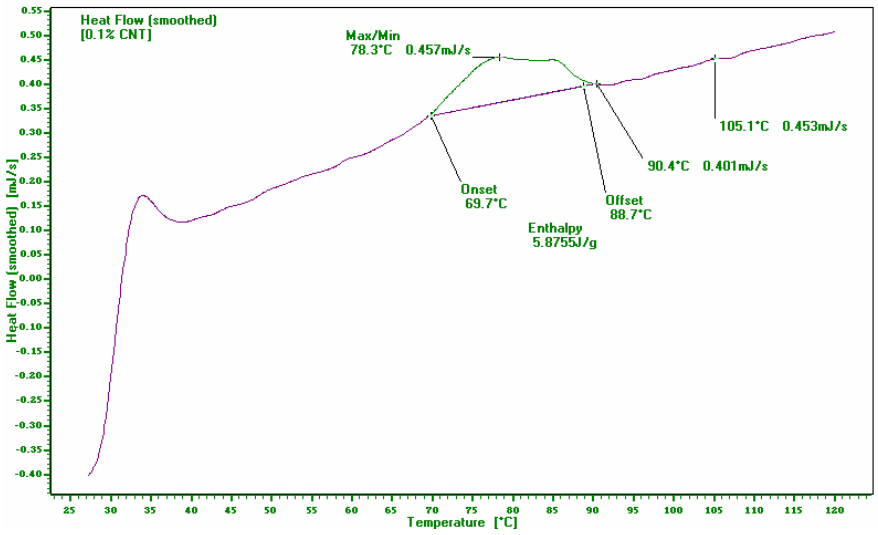

(c)

Fig.3.3 DSC profiles of (a) FLC (b) 0.05% CNTs dispersed FLC (c) 0.1% CNTs dispersed FLC

Figure 3.4 shows the influence of external field on the switching characteristic of FLC and dispersed FLC, at room temperature. The CNT dispersed FLC material shows very fast switching characteristics between two stable states, even at a very small applied voltage of 2 volt. It may be due to induced anisotropic alignment of FLC by CNT in the matrix which could result in the fast switching response.

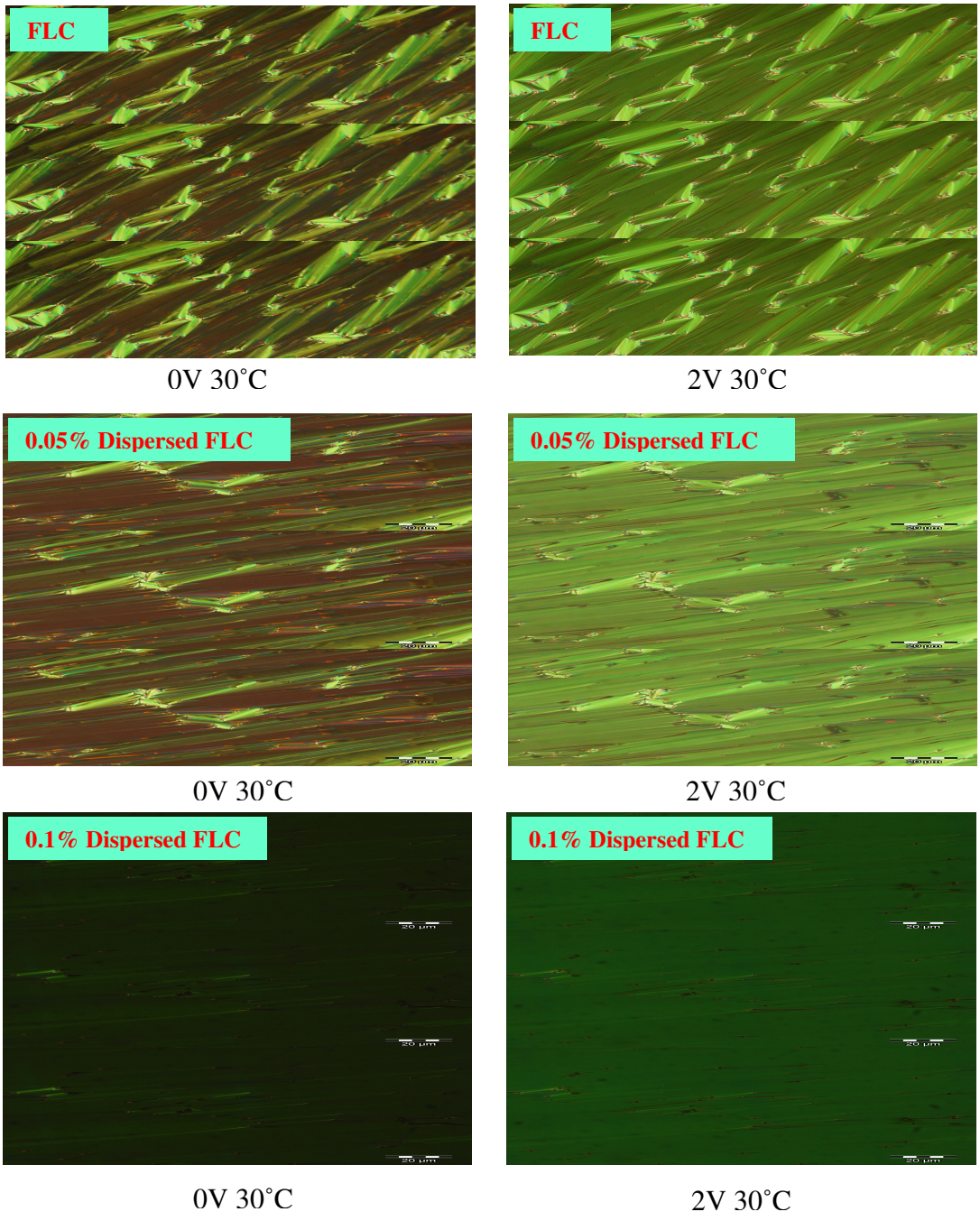

Fig.3.4 Textural variations of the composite films under different field conditions at 30 ^{0}C

3.2 Dielectric spectroscopy

3.2.1 Temperature dependence of dielectric permittivity (ε')

The temperature dependence of dielectric permittivity ε' at different frequencies is shown in Fig 3.5. It was seen that dielectric permittivity attains saturation at about 5 kHz. The

dielectric permittivity value was more predominant at low frequencies (50Hz, 100Hz) however at higher frequencies (above 5 kHz), no significant variation in the dielectric permittivity was observed. The reason behind this behavior was that at higher frequency, liquid crystal dipoles had not sufficient time to align themselves with the direction of applied electric field.

The dielectric permittivity decreases with temperature as shown in fig. 3.5. At high temperature, the thermal agitation became more dominant over intermolecular interactions which resulted in collisions between molecules and hence randomization of dipoles. This randomization results in decreased dielectric permittivity.

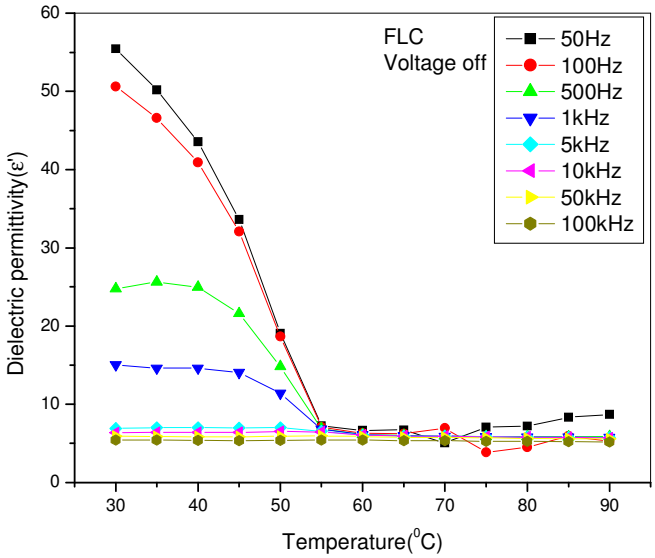

Fig 3.5 Dielectric permittivity (ε') as a function of temperatures at different frequencies without bias voltage.

Fig. 3.6 (a) shows the effect on the dielectric permittivty of MWNT dispersions in ferroelectric liquid crystals at zero biasing and 50 Hz. It was observed that dielectric permittivity increased on dispersing CNT in ferroelectric liquid crystals at lower temperatures but at higher temperatures there was no significant variation in dielectric permittivity values. Such kind of behavior shown by CNT-FLCs composite might be due to the conducting nature of CNT and also they had given alignment to liquid crystal molecules and hence enhanced its dielectric permittivity. Fig 3.6 (b) shows that at higher frequencies, dielectric permittivity decreases on dispersing CNTs in ferroelectric liquid

crystals. As the concentration of CNTs was increased, dielectric permittivity got decreased at higher frequencies.

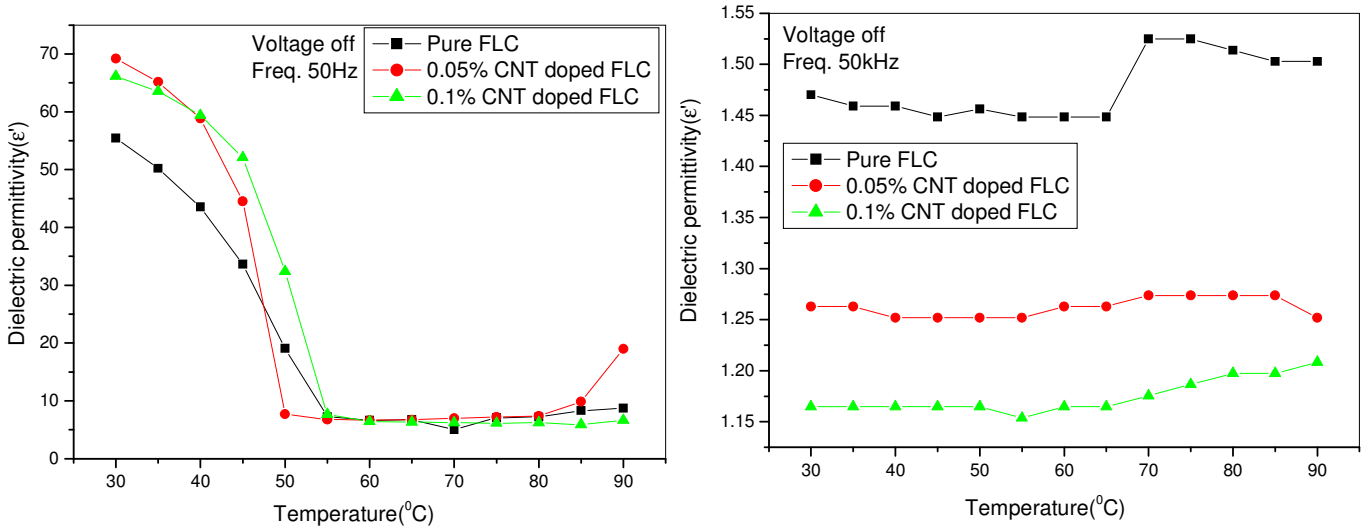

(a) (b)

Fig 3.6 Dielectric permittivity ε' as a function of temperatures for different samples (FLC and CNT dispersed FLC) at (a) 50 Hz (b) 50 kHz.

4.2.2 Frequency dependence of dielectric permittivity and dielectric loss (ε', ε")

Fig 3.7 shows the effect of frequency on dielectric permittivity at different temperatures. The permittivity decreased exponentially up to a frequency of ~2 kHz at all temperatures in the SmC* phase. At higher frequencies dipoles do not show simultaneous response to electric field and hence they do not align along the field direction. Thus dielectric permittivity was decreased on increased frequency. Similar effect was seen at SmA phase except that the values were a smaller.

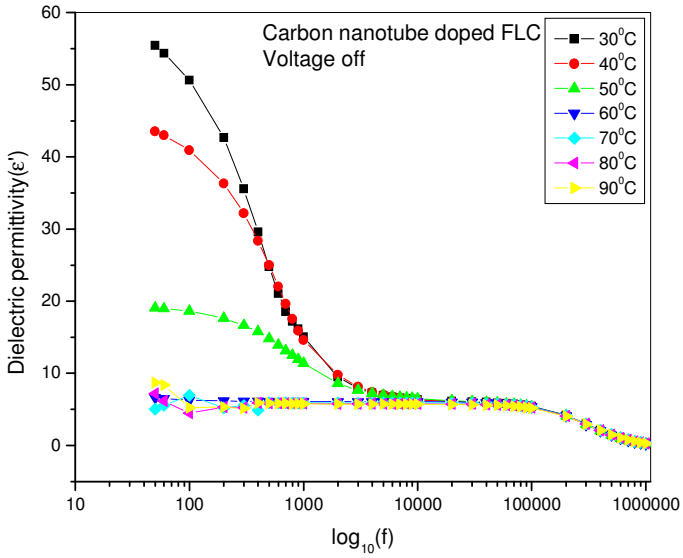

Fig 3.7 Dielectric permittivity ε' as a function of frequency at different temperatures in FLC

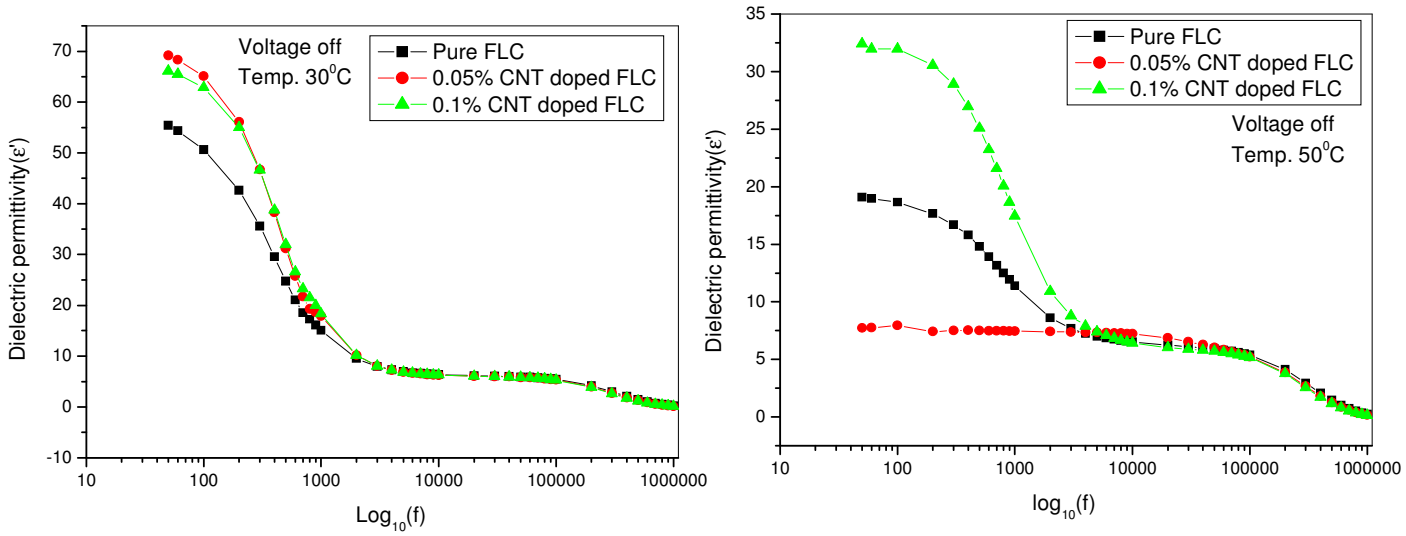

Fig 3.8 Dielectric permittivity ε' as a function of frequency for different samples (FLC and CNT dispersed FLC) at (a) room temperature (b) 50^0C.

Fig 3.8(a) show the effect on the dielectric permittivty of CNT dispersions in ferroelectric liquid crystals at off bias voltage and at room temperature. It was observed that dielectric permittivity got increased on dispersing CNT in ferroelectric liquid crystals at lower

frequencies but at higher frequency there was no significant variation in dielectric permittivity values.

Fig 3.8 (b) shows that at lower frequencies, dielectric permittivity decreases on dispersing 0.05% CNT in ferroelectric liquid crystals but increases on dispersing 0.1% CNT in ferroelectric liquid crystals. The dielectric permittivity is used in calculating the capacitance. Thus ferroelectric liquid crystals give high capacitance values on dispersing the nanotubes in it. Thus makes the FLC applicable for Electronic and memories devices.

Fig 3.9 shows the frequency dependences of dielectric loss (ε") at different temperatures. The dielectric loss was increased from 18 (at 50 Hz) attained a maxima of ~ 26(about 300Hz) at 30^0C and the peak shown was relaxation peak. The maxima in loss were decreased as the temperature increased. At higher frequencies, second loss peak had been observed at about 300 kHz. The origin of this mode is being investigated.

The FLCs shows peak at frequency ~ 300Hz. Peak occurs when the period, 1/ω, it takes to rotate a dipole and do one cycle of work by field is just the time it takes to randomize the orientation and thereby this energy to molecular collision are occur at the same rate and hence energy is being transferred to heat more efficiently.

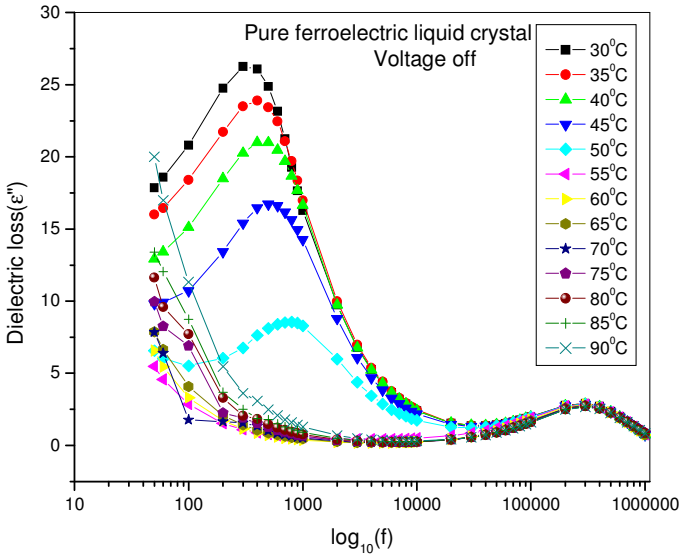

Fig. 3.9 Dielectric loss (ε") as a function frequency at different temperatures

Fig 3.10 shows the effect on the dielectric loss of CNT dispersions in ferroelectric liquid crystals at zero bias voltage and at room temperature. It was observed that dielectric loss was increased on dispersing CNT in ferroelectric liquid crystals at lower frequencies but

at higher frequencies there was no significant variation in dielectric loss. As CNT are conducting in nature, thus on adding the CNT in FLC there should be increased lattice vibration of molecules and hence there would be more dissipation loss. Fig. 3.10 shows the same behavior as defined in theory.

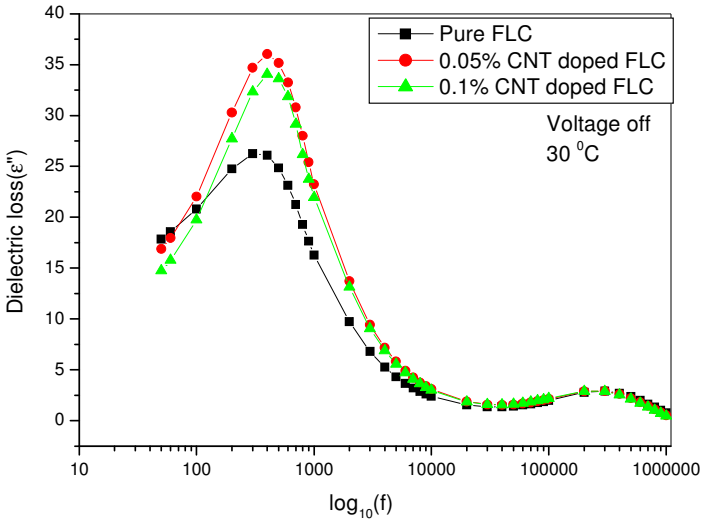

Fig 3.10 Dielectric loss ε" as a function of frequency for different samples (FLC and CNT dispersed FLC) at room temperature.

3.2.3 Relaxation spectra

This relaxation phenomena was also reflected in Cole- Cole plot as shown in fig 3.11. The smaller semi- circle in this figure represents the relaxation due to the Soft Mode where as, bigger semi circle represents the contribution due to Goldstone Mode. In the vicinity of the $T_{c^*\text{-}A,}$ SM followed the Currie-Weiss law. The relaxation frequency (f_i) can be evaluated using an expression

$(v/u) = (\omega\tau)^{1-\alpha}$,

where

$v = [(\varepsilon_0\text{-}\varepsilon'(\omega))^2 + \varepsilon''(\omega)^2]^{1/2}$,

$u = [(\varepsilon'(\omega) - \varepsilon'(\infty))^2 + \varepsilon''(\omega)^2]^{1/2}$,

$\varepsilon'(\omega)$ is dielectric permittivity at particular frequency.

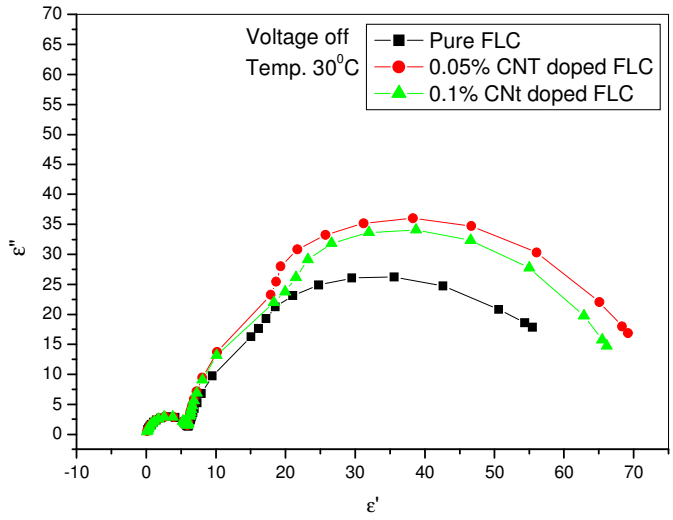

Fig 3.11 Cole-Cole plots for the Goldstone Mode and Soft Mode at different temperature for different mixtures (FLC and CNT dispersed FLC)

4.2.4 Effect of Bias voltage

The dielectric permittivity in SmC* phase was dominant due to the Goldstone mode contribution, so it became difficult to detect the other collective dielectric process. The Goldstone mode can be suppressed by applying a dc bias field, being strong enough to unwind the helicoidal structure. The effect of bias voltage on the Goldstone mode in the form of dispersion is shown in Fig. 3.12(a) and 3.12(b). We saw that the loss was highest without any bias (0V) voltage but decreased with bias voltage e.g. at 10V in the 0.1% CNTs dispersed FLCs. As the biasing voltage increased, dielectric permittivity and dielectric loss were decreased and reached to minimum values. The voltage at which dielectric permittivity and losses become minimum, is called critical voltage. This voltage was sufficient to unwind the helical structure and suppress the Goldstone mode. On increasing the dc bias field, dipoles got strongly aligned and were unable to follow the field. But there was no significant variation in permittivity in FLCs.

On adding the CNTs in FLCs, the molecules got aligned along CNT and were unable to follow the electric field and hence FLC lost their helical structure. Thus dielectric permittivity and dielectric losses got decreased on increasing dc bias field.

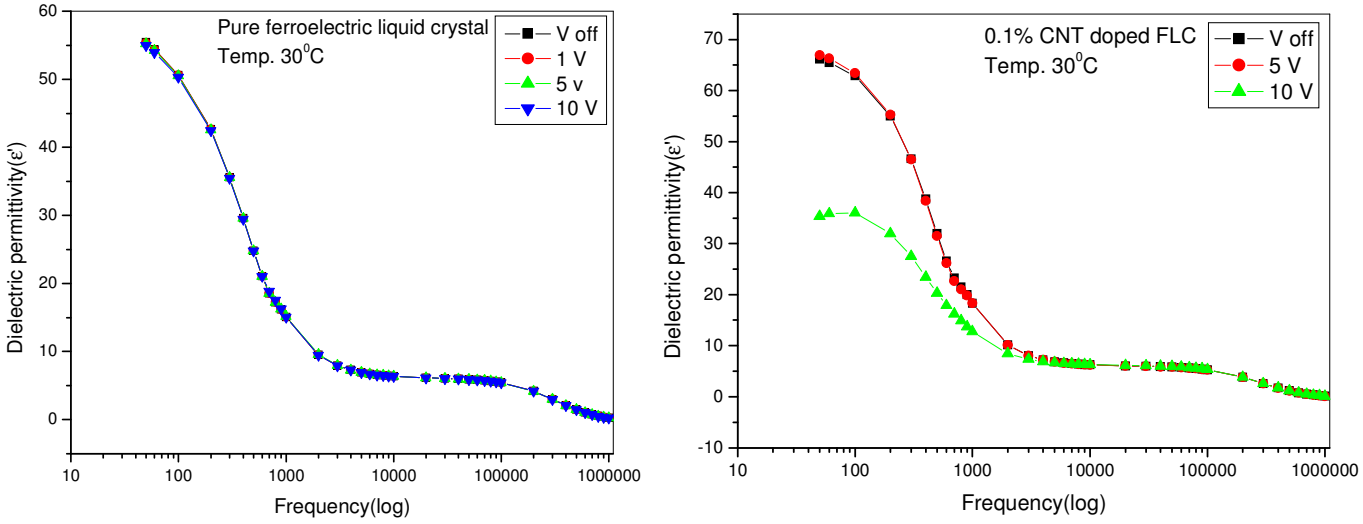

(a) (b)

Fig. 3.12 Dielectric permittivity as a function of frequency at different voltage for (a) FLC (b) 0.1% CNTs dispersed FLC

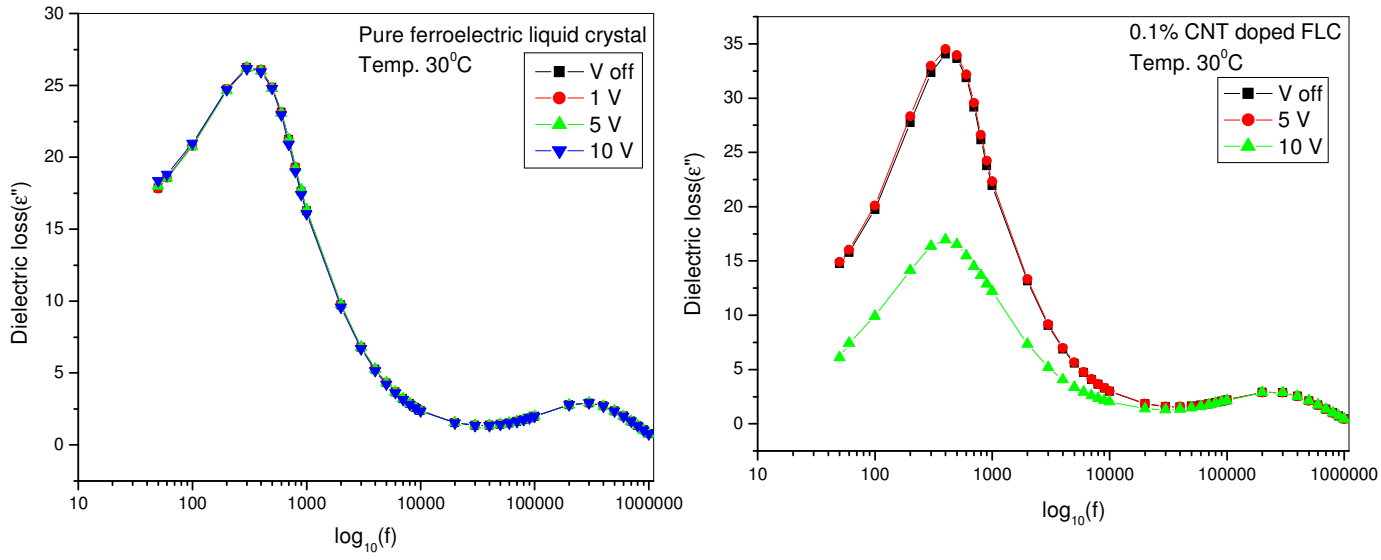

(a) (b)

Fig 3.13 Dielectric loss as a function of frequency at different voltage for (a) FLC (b) 0.1% CNT dispersed FLC

Fig 3.13(a) shows the dielectric permittivity (ε") as a function of frequency at different voltages. It was observed that there was no effect of biasing on FLC. Fig 3.13(b) shows the dielectric permittivity (ε") as a function of frequency at different voltages. Two relaxation peaks at 500Hz and 500 kHz were observable. The first peak corresponds to a domain mode structure where as the second one corresponds to the soft mode. This was also reflected in the form of Cole-Cole plot.

CHAPTER 4
Conclusions

- Our results indicate that by adding a low concentration of nanotubes into a ferroelectric liquid crystal matrix to form composites, have attracted much attention because of their unique morphological and dielectric properties. The effective utilization of CNTs in composite applications strongly depends on the ability to homogeneously disperse them throughout the matrix. However a range of problems also arises in ferroelectric colloidal dispersions. The ferroelectric liquid crystal ordering makes it difficult to suspend small nanotubes in a liquid crystal host. Nanotubes often segregate into agglomerates distributed non-uniformly in the cell. The resulting spatial distribution of the nanotubes is difficult to control. Our research therefore explores the factors that affect the spatial distribution of these nanotubes and thus control morphology of nanotubes– liquid crystal composites.
- It was observed that dispersed nanotubes in FLC, enhanced the alignment of the LC molecules and do not disturb the LC orientation as such. Macroscopically homogeneous structures were obtained, i.e. the suspensions appear similar to a pure LC with no readily apparent evidence of dissolved nanotubes. At the same time the nanotubes are sufficiently large to maintain the intrinsic properties of the materials and share these properties with the LC matrix due to anchoring with the LC. The inherent conductivity and spontaneous self alignment properties of CNTs make them an attractive alternative as an alignment layer.
- We have seen through optical micrographs that there are large CNTs aggregates in the continuum of FLC prepared by simply shaking the compound. We therefore employed sonication of the CNT-FLC mixtures for about 2 hours.
- It is observed that on addition of carbon nanotubes 0.05% and 0.1% wt/wt in FLC, transition temperature increased by 7 ˚C and 17 ˚C respectively.
- The CNT dispersed FLC material shows very fast switching characteristics between two stable states, even at a very small applied voltage of < 2 volt.

- Dielectric permittivity increased by ~ 27% on dispersing CNT in ferroelectric liquid crystals at lower temperatures but at higher temperatures there was no significant variation. Dielectric permittivity increased on dispersing CNT in ferroelectric liquid crystals at lower frequencies but there was no significant variation at higher frequency.
- The dielectric loss increased from 18 attained maxima of ~ 26 when frequency was increased from 50 Hz to 300Hz at 30^0C and the peak shown was relaxation peak. At higher frequencies, second loss peak had been observed at about 300 kHz. It was expected to have been formed as a result of new relaxation mode (NRM).
- On adding the CNTs in FLCs, the molecules of FLC got aligned along CNT and were unable to follow the electric field and hence FLC lost their helical structure. Thus dielectric permittivity and dielectric losses got decreased on increased dc bias field.
- Two relaxation peaks at 500Hz and 500 kHz were observable. They correspond to Goldstone mode and Soft mode respectively as reflected in the form of Cole-Cole plot.

References

1. J. W. Doane., N. A., Wu, B. G. Vaz., And S. Zumer., (1986), Appl. Phys. Lett., 48, 269.
2. M. Kreuzer., T. Tschudi., And R. Eidenschink., (1993), Appl. Phys. Lett., 62, 1712.
3. F. Brochard , And P. G. De Gennes., (1970), J. Phys., 31, 691.
4. B. J. Liang., And S.H. Chen., (1989), Phys. Rev., 39, 1441.
5. Yu. Reznikov., O. Buchnev., O. Tereshchenko., V. Reshetnyak., A. Glushchenko., And J. West., (2003), Appl. Phys. Lett., 82, 1917.
6. Yu. Reznikov, O. Buchnev, O. Tereshchenko, V. Reshetnyak, A. Glushchenko, and J. West. Applied Physics Letters, 82, No 12, 1917-1919 (2003)
7. C. Y. Matuo and A. M. Figueriedo Neto, Phys. Rev. E 60, 1815 (1999).
8. S. Iijima. Nature, 354, 56 (1991).
9. W.A. de Herr, J.-M. Bonard, K. Fauth, A. Chatelain, L. Forro, D. Ugarte. Adv. Mater., 9, 87 (1997).
10. M.D.H. Bockrath, P.L. Cobden, N. McEuen, A. Chopra, A. Zettl, A.R. Thess, R.E. Smalley. Science, 275, 1922 (1997).
11. R.H. Baughman, C. Changxing, A.A. Zakhidov, Z. Iqbal, J.N. Barisci, G.M. Spinks, G.G. Wallace, A. Mazzoldi, D. de Rossi, A.G. Rinzler, O. Jaschinski, S. Roth, M. Kertesz. Science, 284, 1340 (1999).
12. G. Che, B.B. Lakshmi, E.R. Fisher, C.R. Martin. Nature, 393, 346 (1998).
13. P.M. Ajayan, O. Stephan, C. Collix, D. Trauth. Science, 265, 1212 (1994).
14. W.A. de Heer, W.S. Bacsa, A. Chatelain, T. Gerfin, R. Humphreybaker, L. Forro, D. Ugarte. Science, 268, 845 (1995).
15. S. Huang, L. Dai, A.W.H. Mau. J. Mater. Chem., 9, 1221 (1999).
16. C.N.R. Rao, R. Sen, B.C. Satishkumar, A. Govindaraj. Chem. Commun., 1525 (1998).

17. S. Huang, A.H.W. Mau. Appl. Phys. Lett., 82, 796 (2003).

18. S. Huang, L. Dai, A.H.W. Mau. Physica B, 323, 333 (2002).

19. M. Lynch, D. Patrick. Nano Lett., 2, 11 (2002).

20. de Gennes P G and Prost J (1993) The Physics of Liquid Crystals (Oxford: Oxford University Press)

21. P.J.F. Harris, Carbon Nanotubes and Related Structures, Cambridge Univ. Press, Cambridge, UK, (1999).

22. T.W. Ebbesen (Ed.), Carbon Nanotubes: Preparation and Properties, CRC Press, Inc., Boca Raton, (1997).

23. H. Shimoda, S.J. Oh, H.Z. Geng, R.J. Walker, X.B. Zhang, L.E. McNeil,O. Zhou, Adv. Mater. 14 (2002) 899.

24. R. Saito, G. Dresselhaus, M.S. Dresselhaus, Physical Properties of Carbon Nanotubes, Imperial College Press, London, (1998).

25. W. Song, I.A. Kinloch, A.H. Windle, Science 302 (2003) 1363.

26. Dekker, et al. (1999)

27. Poulin P., Raghunathan V.A., Richetti P., and Roux D.: On the dispersion of latex particles in a nematic solution. J Phys II. (1994); 4: 1557-1569.

28. P.J.Colling, Liquid Crystal: Nature's Delicate Phase of Matter, Pricenton: University Press (1990)

29. P. J. Colling and Michael Hird, Introduction to Liquid Crystal: Chemistry and Physics, Taylor and Francis Ltd (1997)

30. S. Chandrasekhar, Liquid Crystal 2nd Edn. Cambridge: Cambridge University Press (1992)

31. P. G. De Gennes, The Physics of Liquid Crystal: Oxford University Press (1975)C. Khoo, Physics of Liquid Crystalline Materials (Amsterdam: Golden and Breach) (1991)

32. R.B.Meyer, L. Liebert, P.J.Killer, J. Phys. (Paris) Lett. 36 (1995) L-69.

33. L.A. Beresnev, L.M. Blinov, M.A. Osipore, S.A. Pikin, Mol. Cryst. Liq. Cryst. A. 3 (1988) 158.

34. C.Filipic, T. Carlsson, A. Levstik, B. Zeks, R. Blinc, F. Gouda, S.T. Lagerwall, K. Skarp, Phys. Rev. A 38 (1988) 5833.

35. A.M. Biradar, S. Wrobel, W. Hasse, Phys. Rev. A 39 (1989) 2693.

36. S. Hiller, A.M. Birader, S.Wrobel, W. Hasee, Phys. Rev. E 53 (1996) 641.

37. Arvind K. Gathania, Buta Singh, K.K. Raina, J.Phys. Condens, Matter 11 (1999) 3813.

38. K.K.Raina, Jassjit K Ahuja, Mol. Cryst. Liq. Cryst. 325 (1998) 157.

39. A.M. Birader, S.S. Bawa, W. Haase, Ferrolectrics 256 (2001) 201.

40. A.M. Birader, S.S. Bawa, C.P. Sharma, Subhas Chandra, Ferroelectrics 122 (1991) 81.

41. K. Kondo, T. Kitamura, M. Isogai, A. Mukoh, Ferroelectrics 132 (1988) 99.

42. S. Wrobel, G. Cohen, W. Haase, M. Marzec, M. Pfeiffer, Ferrolectricc 166 (1995) 211.